Heliyon 8 (2022) e11384

Contents lists available at ScienceDirect

Heliyon

journal homepage: www.cell.com/heliyon

Research article

Ozone pollution in London and Edinburgh: spatiotemporal characteristics, trends, transport and the impact of COVID-19 control measures

Cristiana Tudor *

International Business and Economics Department, Bucharest University of Economic Studies, 010374 Bucharest, Romania

ARTICLE INFO

Keywords:
Air pollutants
Trend estimation
Theil-Sen estimator
Mann-Kendall test
Generalized additive model
Trajectory analysis
COVID-19 lockdown impact
Ozone pollution
London
Edinburgh

ABSTRACT

Air pollution remains the most serious environmental health issue in the United Kingdom while also carrying non-trivial economic costs. The COVID-19 lockdown periods reduced anthropogenic emissions and offered unique conditions for air pollution research. This study sources fine-granularity geo-spatial air quality and meteorological data for the capital cities of two UK countries (i.e. England's capital London and Scotland's capital Edinburgh) from the UK Automatic Urban and Rural Network (AURN) spanning 2016–2022 to assess long-term trends in several criteria pollutants (PM10, PM2.5, SO2, NO2, O3, and CO) and the changes in ozone pollution during the pandemic period. Unlike other studies conducted thus far, this research integrates several tools in trend estimation, including the Mann-Kendall test, the Theil-Sen estimator with bootstrap resampling, and the generalized additive model (GAM). Moreover, several investigations, including cluster trajectory analysis, pollution rose plots, and potential source contribution function (PSCF), are also employed to identify potential origin sources for air masses carrying precursors and estimate their contributions to ozone concentrations at receptor sites and downwind areas. The main findings reveal that most of the criteria pollutants show a decreasing trend in both geographies over the seven-year period, except for O3, which presents a significant ascending trend in London and a milder ascending trend in Edinburgh. However, O3 concentrations have significantly decreased during the year 2020 in both urban areas, despite registering sharp increases during the first lockdown period. In turn, these findings indicate on one hand that the O3 generation process is in the VOC-limited regime in both UK urban areas and, on the other hand, confirm previous findings that, when stretching the analysis period, diminishing ozone levels can lead to NOx reduction even in VOC-controlled geographies. Trajectory analysis reveals that northern Europe, particularly Norway and Sweden, is a principal ozone pollution source for Edinburgh, whereas, for London, mainland Europe (i.e., the Benelux countries) is another significant source. The results have important policy implications, revealing that effective and efficient NOx abatement measures spur ozone pollution in the short-term, but the increase can be transient. Moreover, policymakers in London and Edinburgh should consider that both local and transboundary sources contribute to local ozone pollution.

1. Introduction

Pollution is defined as the contamination of the environment caused by the presence of substances in the atmosphere that are harmful to the health of humans and other living beings (Manisalidis et al., 2020). Thus, air pollutants are natural and artificial airborne substances that are discharged into the environment in a concentration sufficient to have a measurable effect on humans, animals, vegetation, or building supplies (Lois et al., 2022). Many characteristics distinguish air pollutants, including their chemical nature, reactivity, emissions, persistence in the environment, ability to be dispersed over long or short distances, and subsequent effects on human health and/or the environment (Fino, 2019). Two main categories of air pollutants are gaseous pollutants, which are mainly attributed to the combustion of fossil fuels and comprise SO2, NO2, CO, and O3, and particulate matter (PM), generated by a wide range of natural and man-made sources, that include PM10 (i.e., coarse) and PM2.5 (i.e. fine) particulate matter. As part of national and international regulatory processes, most common air pollutants have become “criteria pollutants”, whereby regulatory agencies set air quality standards for them based on criteria ((NHDES, 2022) and that serve to determine if a geography's air quality standards are met (Vallero, 2014).

* Corresponding author.
E-mail address: cristiana.tudor@net.ase.ro.

https://doi.org/10.1016/j.heliyon.2022.e11384
Received 18 July 2022; Received in revised form 21 September 2022; Accepted 28 October 2022

Air pollution remains a major environmental risk to human health (Mendes et al., 2022), causing an estimated 7 million premature deaths each year (WHO, 2021), which surpasses more than five times the number of persons killed in traffic accidents and exceeds the official COVID-19 death count ((UNEP, 2021). Moreover, despite an increase in legislation and regulations aimed at combating air pollution, air quality continues to deteriorate (UN, 2021), and nine out of ten people worldwide breathe air with pollution levels that surpass World Health Organization guidelines. In particular, in 2019, 99 percent of the world's population lived in areas where WHO air quality requirements were not met. Moreover, air pollutants such as particulate matter (PM), NO2, and O3 are acknowledged as significant risk factors for cardiovascular and respiratory disorders, and drivers of global mortality (Sheng and Tang, 2013; Lee et al., 2017). Additionally, the economic costs of air pollution are severe, with estimates indicating 5 trillion USD in welfare losses and 225 billion USD in lost revenue (WMO, 2020; World Bank Institute for Health Metrics and Evaluation, 2016). According to the OECD (2021), the overall annual market costs of outdoor air pollution are expected to climb from 0.3 percent in 2015 to 1.0 percent by 2060.

As of 2018, the UK ranks 15th among the world's top polluters in absolute terms (Tudor and Sova, 2021). Consequently, air pollution is the most serious environmental health issue in the United Kingdom, with outdoor pollutants reported to cause between 28,000 and 36,000 premature deaths per year (Public Health England, 2019), costing the UK economy up to £20 billion every year (ADPH, 2017). However, there is heterogeneity in air quality across the UK, with a clear South/North divide to the problem (Centre for Cities, 2020). London is one of the most polluted areas in the United Kingdom and it is currently the most important geography failing to meet the legally binding limits for main air pollutants imposed at the European Union level (London Air, 2022), also surpassing WHO air pollution limits (Air quality news, 2022). Moreover, Scotland reports on average superior air quality than England and the rest of the United Kingdom (The Scotsman, 2022a). As such, while the majority of state governments in the UK adhere to the European Union's minimum air quality guidelines, which for PM2.5 levels is 25 g/m^3 yearly exposure, air quality in Scotland is kept to a significantly lower limit of 10 g/m^3, which conforms to the WHO benchmark (IQAir, 2022). However, the capital city of Edinburgh still exceeds the target limit concentration of nitrogen dioxide on a yearly basis and ranks second to worst among major European cities in terms of air pollution improvements (The Scotsman, 2022b). However, the spatial scale of air pollution concerns can vary substantially, ranging from local (i.e., restricted environmental impact) to regional in character. Furthermore, the temporal scale of air pollutant problems can also differ, from accidental discharges of high pollutant concentrations, which may have an immediate impact on biodiversity and may result in a delayed and gradual recovery, to the accumulation of pollutant buildup over years or decades (Ashmore, 2013). Furthermore, it should be noted that meteorology is a critical factor in the re-distribution of airborne pollutants once they are released into the atmosphere (Boubel et al., 2013), and thus, meteorological factors should be considered for accurate air quality modeling and forecasting.

Given the above considerations, there is a dire need for more research on the accurate characterization, estimation, and prediction of air pollutants, based on high-resolution geospatial data, that could offer relevant information for identifying efficient policies and control measures to improve air quality and ultimately mitigate pollution-caused health problems and economic costs (Tudor and Sova, 2022). Additionally, such studies are important contributors to addressing the triple global crisis of climate change, biodiversity loss, and pollution and waste (UN, 2021). All these factors are, in turn, significant motivators for this research. Concurrently, the lockdown imposed during the COVID-19 pandemic by many nations around the globe, including the UK, constitutes a perfect opportunity (Mahato et al., 2020) for assessing the impact of restricted human activities on air quality in urban centers. The COVID-19 pandemic's effects on air pollution are deemed impossible to reproduce outside of this worldwide health emergency (Campbell et al., 2021), which further motivates our research endeavor. A plethora of media sources reported significant improvements in air quality as a result of pandemic-related unprecedented reductions in anthropogenic activity (among others, CNN, 2020; World Economic Forum, 2020; Washington Post, 2020). Concurrently, academic research increasingly documented that containment measures had a positive impact on air quality (Saadat et al., 2020; Dantas et al., 2020; Tobias et al., 2020; Siciliano et al., 2020; Venter et al., 2020). In particular, the media and the academic community focused on the reduction in NO2 and other primary pollutants as proof of air quality improvement (Wang and Su, 2020; Siciliano et al., 2020; Pey and Cerro, 2022). According to estimates by the Centre for Research on Energy and Clean Air, the declines in NO2 and particulate matter (PM) that occurred across Europe following the implementation of pandemic-control measures mitigated the number of air-pollution related deaths by 11,000 in 30 days (Myllyvirta and Thieriot, 2020). These estimates, however, do not account for variations in concentrations of secondary pollutants, which frequently pose a greater threat to human health than some primary species (Wyche et al., 2021). In particular, the decline in ambient NOx concentrations (*i.e.,* NO + NO2) impacts the levels of ozone (O3) (Wyche et al., 2021), a secondary atmospheric pollutant produced through the interaction of sunlight with NOx and volatile organic compounds (VOC) (Lee et al., 2014; Siciliano et al., 2020; NRCS, 2022; EEA, 2022). Reactions have generally been assumed to be heat and sunlight-dependent, resulting in increased ambient ozone concentrations during the summer months (EPA, 2022). However, the majority of ground-level ozone is produced by the reaction of anthropogenic VOC and NOx, although some stratospheric ozone is transferred into the troposphere (Chen et al., 2022) and some levels of VOC and NOx do exist naturally (EPA, 2021). Consequently, nonlinear photochemistry governs the interaction between ozone, VOC, and NOx, and O3 formation's sensitivity to VOC and NOx is highly uncertain (Dantas et al., 2019; Querol et al., 2021). Moreover, it has been shown that ozone production is not always directly proportional to the concentrations of its precursors (namely VOC and NOx) (Pusede and Cohen, 2012; Pusede et al., 2014), and in turn, three distinct regimes for ozone production have been delineated: NOx limited (low NOx and high VOC), NOx saturated (high NOx and low VOC), and transitional (Balamurugan et al., 2022). The three regimes and their different behaviors to changes in the VOC/NOx balance further contribute to explaining part of the divergent findings of previous studies concerning the effects of COVID-19 pandemic containment measures on ozone pollution. Thus, in a study that encompasses alternative O3 generation regimes throughout Europe, Cuesta et al. (2021) have explored the pandemic impact on ozone concentrations during 1–15 April 2020 and reported positive changes in VOC-limited regimes and negative changes in areas where NOx drives ozone chemistry.

Specifically, the COVID-19 epidemic caused significant reductions in NO emissions, with a subsequent magnifying effect on O3 concentrations in VOC-limited regions (Rahman et al., 2021). This link has been further confirmed by other studies that documented increased ozone pollution in the aftermath of the pandemic outbreak in distinct geographies (among others, Ordóñez et al., 2020; Petetin et al., 2020; Tobias et al., 2020; Sicard et al., 2020a,b; Xu et al., 2020; Sulaymon et al., 2021; Torkmahalleh et al., 2021; Gopikrishnan et al., 2022). Few studies have performed this analysis for the UK, focusing on London (Zhang and Stevenson, 2022) or the South East of the UK (Wyche et al., 2021), while the UK-wide research remains thin (Lee et al., 2020). Most importantly, most of the aforementioned investigations are limited to the short span of the first pandemic wave (Lee et al., 2020; Wyche et al., 2021) and thus do not assess the longer-range impact of the enforcement of lockdown periods as a response measure to the COVID-19 pandemic. Moreover, specific investigations into ozone pollution in Scotland and the changes in air quality in the aftermath of the pandemic outbreak remain unaccomplished, to the best of the author's knowledge. Given that ozone pollution can rise if restrictions are applied to the improper precursor

(Rahman et al., 2021), considering UK-wide legislation aimed at ceiling emissions of air pollutants, including oxides of nitrogen (UK Legislation: National Emissions Ceiling Regulations, 2018, https://www.legislation.gov.uk/uksi/2018/129/contents/made), and acknowledging the health impact of ozone pollution, the relationship is of paramount importance to policymakers, which motivates the current research. Of note, it has been suggested that a weakening of titration following the significant drop in NO concentrations, especially during the first pandemic wave, as well as the proportionally greater total NOx decrease relative to total non-methane hydrocarbons, explain the rise in O3 levels in Asian and European urban regions (Wyche et al., 2021). However, other factors should be considered, including the origin of air masses, when analyzing the spatiotemporal behavior of air pollutants in urban areas with a complicated pattern of pollution sources and/or during special periods when the sources' contribution is massively affected (Siciliano et al., 2020).

In light of these considerations, the objectives of the present study and its main contributions to the extant literature are to (i) assess pollutants' long-term trends in the capital cities of two UK countries (i.e. England's capital London and Scotland's capital Edinburgh); (ii) assess the impact of lockdown on O3 pollution in the two urban centers, and (iii) assess the long-range transport impact and reveal potential origin sources for ozone pollution in the capital cities of England and Scotland. Of note, this study goes further than previous studies to examine trends and variability of O3 concentrations in the two urban centers. As such, long-term trends are produced by alternative methods, specifically the Theil-Sen estimator, Mann-Kendall test, and bootstrap resampling, as well as the Generalized Additive Model (GAM), ensuring the robustness of results. Several investigations, including cluster trajectory analysis, pollution rose plots, and potential source contribution function (PSCF), are also employed to identify the origin sources for air masses carrying precursors and estimate their contributions to ozone concentrations at receptor sites and downwind areas.

The remainder of this paper continues as follows. Section two presents and discusses the data and the methods employed to perform the investigation. Empirical results are presented in Section three, while Section four contains a discussion of the findings. The final section concludes the research.

2. Materials and methods

2.1. Data

This study sources high-resolution hourly information from the Automatic Urban and Rural Network (AURN) (website: https://uk-air.defra.gov.uk/networks/network-info?view=aurn), the UK's largest automatic monitoring network and also the main network used for compliance reporting against the Ambient Air Quality Directives. Specifically, we retrieve hourly average concentrations of six main "criteria" pollutants (PM10, PM2.5, SO_2, NO_2, O_3, and CO) measured by the ambient air quality monitoring stations located in Central London (i.e., London Marylebone Road) and Edinburgh (i.e., Edinburgh St Leonards), as per Figure 1. AURN employs a range of monitoring methods, including chemiluminescence (for measuring NO2 concentrations), UV absorption (for O3), and UV fluorescence (for SO2), whereas several DEFRA-approved methods (i.e. Department for Environment, Food and Rural Affairs) are used for PM measurements (all methods can be retrieved from: https://uk-air.defra.gov.uk/networks/monitoring-methods?view=mcerts-scheme).

Moreover, meteorological data (wind direction, wind speed, and air temperature) measured by the two stations are additionally extracted and used in various analysis methods (i.e., wind and pollution rose plots, potential source contribution function (PSCF)), providing relevant policy information. Additionally, the meteorological data serves as a control in assessing the potential change in air pollutant concentration trends amid the COVID-19 lockdown periods.

The analysis period spans 16.01. 2016, 00.00:00–11.07.2022, 15.00:00, and includes 114,400 hourly observations for each pollutant and meteorological variable. Table 1 provides more details on the two air quality monitoring stations and highlights all variables employed in this study.

2.2. Historical trends in pollutant concentrations in London and Edinburgh

Figure 2 shows the evolution of the main air pollutants (PM10, PM2.5, SO_2, NO_2, O_3, CO, and benzene) in the two UK urban centers over the entire analysis period spanning 2016–2022 (Figure 2). The air quality in London has seen an overall improvement, with PM10 levels dramatically reduced over recent years, whereas Edinburgh does not register decreases in pollutant concentrations, thus confirming its inclusion among major European cities with the least improvements in air quality. Moreover, a discrepancy in absolute levels of pollutant concentrations between the two cities is noticed, with pollutant concentration levels measured in London (i.e. for PM10) approximately three times higher than the levels registered in Edinburgh over the same period. This in turn provides relevant insight for subsequent investigations, suggesting that pollutant levels must be normalized to allow for the direct comparison of variables using the same scale and that the slope parameters that emerge from trend estimations should be expressed as annual percentage changes for robust inference.

2.3. Method

2.3.1. Bivariate polar plots

Bivariate polar plots have proven to be particularly useful for identifying and comprehending air pollution sources (Carslaw et al., 2006; Westmoreland et al., 2007). Specifically, the wind speed dependency of a source can reveal essential information about its type and properties (Jones et al., 2010; Carslaw and Ropkins, 2012a, 2012b). For example, the wind rose plots are histograms that show the joint relative frequency of wind speed and direction at a particular location (Applequist, 2012; Roubeyrie and Celles, 2018). In this study, the windRose function within R' "openair" package is called. Of note, the function carries the non-trivial advantage of correcting for bias in generating wind roses (see Droppo and Napier (2008) and Applequist (2012) for more details). Thus, the function is able to correct for bias by globally rescaling the count in each wind direction bin by the number of directions it represents relative to the average (Carslaw, 2022).

Additionally, pollution rose plots are useful tools for analyzing pollutant concentrations by wind direction and can offer particularly relevant information (Henry et al., 2009; Carslaw, 2022). As per Munn (1969), pollution roses reveal two important pieces of information: the associated air quality for each wind direction and the distribution and strength of emission sources in the measurement station area. In this study, we draw both wind and pollution roses to identify and quantify the impact of possible source regions of alternative air pollutants as identified by distinct wind direction sectors in the two geographies. This further aids in controlling the impact of the meteorological variables on pollutant trends and thus increases the robustness of the results. Furthermore, to gain valuable insight into the wind directions that most contribute to overall air pollutants concentrations, we highlight the proportional contribution to the mean when drawing pollution rose plots.

2.3.2. Back-trajectory and spatial source analysis

The back-trajectory analysis can detect the likely sources and transport routes for air masses and has thus been frequently employed to assess the long-range transport impact on air pollution (Makra et al., 2013; Hao et al., 2019; Bodor et al., 2020). One of the most widely used tools to generate backward trajectories in given starting locations is the NOAA HYSPLIT model (Hybrid Single Particle Lagrangian Integrated Trajectory Model) (NOAA, 2022: https://www.ready.noaa.gov/HY

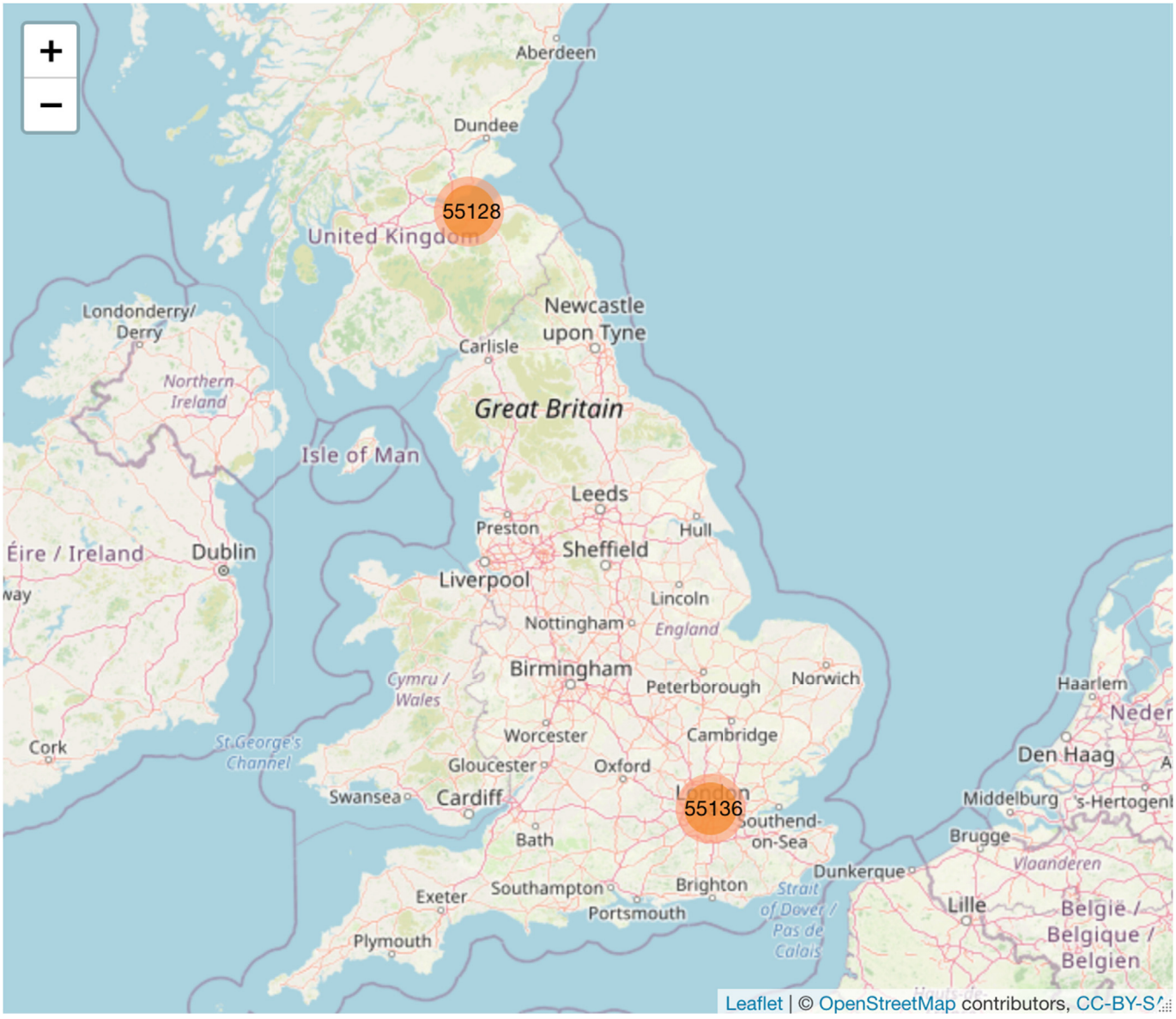

Figure 1. Location of the two UK air monitoring stations. Author's representation in R software with "leaflet" package for creating interactive spatial maps (see Earth Lab, 2022 for more details).

SPLIT.php) (Su et al., 2015). Stein et al. (2015) offer relevant details about the HYSPLIT model.

In this study, the back trajectory data for London and Edinburgh are sourced by calling the importTraj () function within the "openair" package in R software to import pre-calculated back trajectories using the NOAA HYSPLIT model. Of note, 96-hour back trajectories arriving at the two measurement sites are run at 3-hour intervals. Additionally, the trajectories are propagated backward in time and begin at ground level (10 m) (Carslaw, 2022).

Moreover, back trajectories are subsequently classified via the cluster analysis (CA) statistical approach. Consequently, six clusters have been delineated. As per Anil et al. (2017), the spatial variance (SV) between each endpoint (k) along the trajectory (j) within its cluster (i) is estimated as in Eq. (1):

$$SV_{i,j} = \sum_{k} \left(P_{j,k} - M_{i,k}\right)^2 \quad (1)$$

where P and M are the location vectors for the individual trajectory and its cluster mean trajectory, respectively, and the sum is calculated across the number of endpoints along the trajectory. Then, the total spatial variance of all trajectories within a cluster makes up the cluster spatial variance (CSV), and finally, the sum of the CSVs across all clusters gives the total spatial variance (TSV) as in Eq. (2):

Table 1. Details of the air monitoring stations in London and Edinburgh and research variables.

Site	Code	Latitude	Longitude	Air pollutants	Meteorological data	No observations (hourly)
London Marylebone Road	MY1	51.52253	-0.154611	PM10, PM2.5, SO2, NO2, O3, CO	Air temperature, wind direction, wind speed	57209
Edinburgh St Leonards	ED3	55.94559	-3.182186	PM10, PM2.5, SO2, NO2, O3, CO	Air temperature, wind direction, wind speed	57192

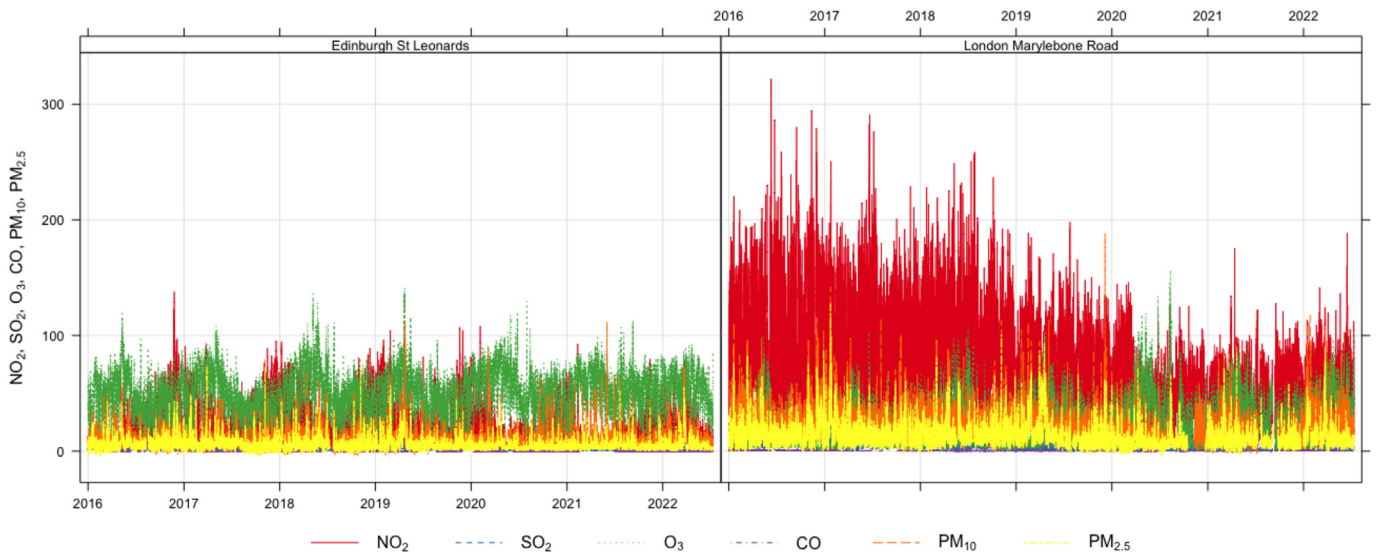

Figure 2. Time series evolution for main air pollutant concentrations in London and Edinburgh over 2016–2022.

$$TSV = \sum_{i} CSV_{j,k} \tag{2}$$

For the current investigation, the trajCluser () function within R's "openair" package is called to cluster the HYSPLIT back trajectories by using an angle-based distance matrix based on Sirois and Bottenheim (1995). The next step consists of merging the cluster and measurement data and assessing how pollutant concentrations vary per cluster.

Furthermore, the Potential Source Contribution Function (PSCF), frequently used in the analysis of air mass back trajectories (Carslaw, 2022), is employed to assure the robustness of the trajectory analysis. PSCF has been acknowledged as a useful tool for trajectory analysis and source identification (Jeong et al., 2011; dos Santos and Hoinaski, 2021), and is given by Eq. (3):

$$PSCF = \frac{m_{ij}}{n_{ij}} \tag{3}$$

where n_{ij} reflects how many times the trajectories went through the cell (i,j) and m_{ij} indicates how many times a particular source concentration was high (i.e., m_{ij} is controlled by "percentile" within the function) when the trajectories went through the respective cell.

2.3.3. Trend analysis

The trend of pollutant concentrations is further explored by employing the Theil-Sen estimator (Theil, 1950; Sen, 1968), also known as the Kendall robust line-fit method. The method is acknowledged as robust for linear regression as it calculates the median slope among all lines using pairs of two-dimensional sample points (Tilgenkamp, 2022). The Theil-Sen estimator is thus a non-parametric median-based estimator that provides additional benefits over standard methods: (i) it issues accurate confidence intervals with non-normal and heteroskedastic data; and (ii) it is resistant to outliers, which could have increased relevancy for air pollution data (Carslaw, 2022). Furthermore, it has been found that the estimator competes well against OLS for normally distributed data in terms of statistical power (Wilcox, 2001).

Hence, the slopes of all possible $\frac{n}{2} = \frac{n(n-1)}{2}$ combinations of pairs of points are estimated and the non-parametric slope is the spatial median of these slopes, as follows in Eq. (4) (Chervenkov and Slavov, 2019):

$$\widehat{\beta}_1 = median\{\tilde{B}\}, \tilde{B} = \left\{ b_{ij} \middle| b_{ij} = \frac{y_j - y_i}{x_j - x_i}, x_i \neq x_j, 1 \leq i < j < n \right\} \tag{4}$$

The Mann–Kendall test is recommended by the World Meteorological Organization (WMO) and has been widely employed for evaluating trends in hydro-climatic studies (Ali et al., 2019).

All estimations are performed in R software, particularly the "openair" package. A non-trivial advantage provided by the "TheilSen" function in the "openair" package is that the robustness of estimates is increased through bootstrap resampling. Consequently, when calling the function, multiple simulations are performed to check the uncertainty in the slope. Moreover, in light of the exploratory analysis of data, which revealed important discrepancies in absolute pollutant concentration levels between the two urban centers, all slope parameters are expressed as annual percentage changes. The function allows this specification through the "slope.percent" option. Furthermore, all trend estimates emerge from de-seasonalised time-series, which in turn is accomplished by calling the "stl" function ("stats" package) to perform seasonal decomposition by loess (Cleveland et al., 1990).

Finally, to assure the robustness of trend estimates, the generalized additive model (GAM) (Hastie, 2017) that extends traditional generalized linear models (GLM) (Dominici et al., 2002) and provides greater flexibility in analyzing non-normal data (Ravindra et al., 2019) is also employed. Owing to its non-trivial advantages, GAM has been increasingly applied in environmental research (Jacob and Winner, 2009; Ravindra et al., 2019). As per Cheng et al. (2021), a basic GAM model is given by Eq. (5):

$$g[E(Y)] = \varepsilon + f_1(X_1) + f_2(X_2) + f_3(X_3) + \ldots + f_n(X_n) \tag{5}$$

where E(Y) denotes the expectation of the response variable Y, g () is the connection function, Ɛ stands for the intercept, X_n are the explanatory variables, and f_1 to f_n refer to regression spline functions.

Consequently, GAM models that include both trends and seasonal variations in pollutant concentrations are estimated for each site through the gam () function in R's "mgcv" package. Wood (2017) offers relevant details on GAM implementation in the R environment.

3. Results

3.1. Variations in meteorological conditions

First, we assess whether there are significant differences in the wind direction in the two urban centers over the 7-year period. Appendix A.1 reflects the wind speed and direction frequencies by year in London (panel a) and Edinburgh (panel b), where the scale in each panel shows the intervals that the wind speed is split into. It emerges that there are no

significant differences between the years within the same area, but some interesting discrepancies emerge between the two urban centers: while the wind rose graphic tool identifies that SW is the "predominant" wind direction in London, it also highlights that westerly winds dominate in Edinburgh, whereas wind speed in Edinburg is higher than in the Central London area.

Moreover, the variation in temperature in the two urban sites is reflected in Appendix A.2, which confirms that yearly patterns in temperature are similar over the seven years.

3.2. Back trajectory and spatial source analysis

The cluster analysis on back trajectories in the two urban centers is reflected in Figure 3 (a,b) (which show six clusters) and further indicates that in both geographies the majority of the back trajectories originated from the Atlantic over the analysis period, although northern Europe is also a significant source.

However, as the trajectory analysis only tells part of the story, a more relevant approach is to merge the cluster and measurement data and subsequently analyze how pollutant concentrations vary per cluster. Consequently, Table 2 contains summary results in the case of ozone, highlighting that for London, mean concentrations of ozone show large variations within the six clusters, whereas less variation is encountered for Edinburgh. For example, cluster 5 in the case of London and cluster 4 for Edinburgh are associated with the highest concentrations of ozone. Of note, both of these clusters originate from Northern Europe.

Next, the pollution rose plots depicted in Figure 4 complement the analysis by highlighting pollutant concentrations by wind direction in London (panels a, c, e) and Edinburgh (panels b, d, f). For space reasons, we present pollution roses for the two criteria pollutants that are known to surpass mandatory targets in the two cities, i.e., PM10 and NO2, and also for ozone, for reasons that pertain to the subsequent investigation. The visual inspection of the six pollution rose plots reveals the dominance of south-westerly winds in controlling the overall mean concentrations of PM10 (panel a) and NO2 (panel c) in Central London, as well as the dominance of westerly winds on mean levels of PM10 (panel b) and NO2 (panel d) in Edinburgh over the 2016–2022 analysis period. Hence, 30% of the nitrogen dioxide concentration (panel d) and over 20% of PM10 (panel b) and O3 (panel f) concentrations in Edinburgh are contributed by the west wind sector, whereas approximately half of the overall PM10 and NO2 concentrations in central London are contributed by three wind sectors in the southwest. However, although most parts of the concentrations are associated with the west and southwest sectors, it should be acknowledged that in both geographies, the highest concentrations of PM10 and ozone are in fact determined by the north-easterly wind sectors. Additionally, for London, north-easterly winds are also associated with the majority of O3 concentrations (panel e).

Table 2. Ozone concentrations per cluster.

Cluster	London	Edinburgh
C1	16.6	46.4
C2	16.6	45.4
C3	12.4	42.0
C4	18.2	51.7
C5	30.4	46.1
C6	30.3	40.5

Figure 5 reflects the PSCF plot for ozone for concentrations' 90th percentile in London (panel a) and Edinburgh (panel b) and reinforces that the principal ozone sources are dominated by source origins in northern Europe, particularly Norway and Sweden in the case of Edinburgh, and also mainland Europe (i.e., the Benelux countries) in the case of London.

3.3. Long-term trend analysis

For a clear reflection of the 7-year trends in pollutant concentrations in the two UK capital cities, the data is normalized. Consequently, annual means are first estimated, and indexation to 100 at the beginning of 2016 is subsequently accomplished. Figure 6 reflects the trends of normalized criteria pollutants in London (panel a) and Edinburgh (panel b) and reveals that concentrations of O_3 have more than doubled in London over the period 2016–2022, whereas SO_2 and NO_2 have shown the greatest reductions (by approximately 50%). In Edinburgh, the trends of normalized pollutant levels reveal that O_3 concentrations have also increased over the analysis period, although to a lower extent than in London (approximately 20%). On the other hand, in Edinburgh, CO concentrations have shown the greatest reductions, equaling almost 70%, whereas NO_2 concentrations have decreased by approximately 30%. Interestingly, a disaggregation occurs between London and Edinburgh as far as the trend of SO_2 concentrations is concerned, which presents a very volatile trend over the sample period in Edinburgh and a decreasing trend in London during the same period.

The results of the Theil-Sen trend estimations for all criteria pollutants over the entire sample period (i.e., 2016–2022) are visually presented in Figure 7, which also reveals the de-seasonalized monthly mean

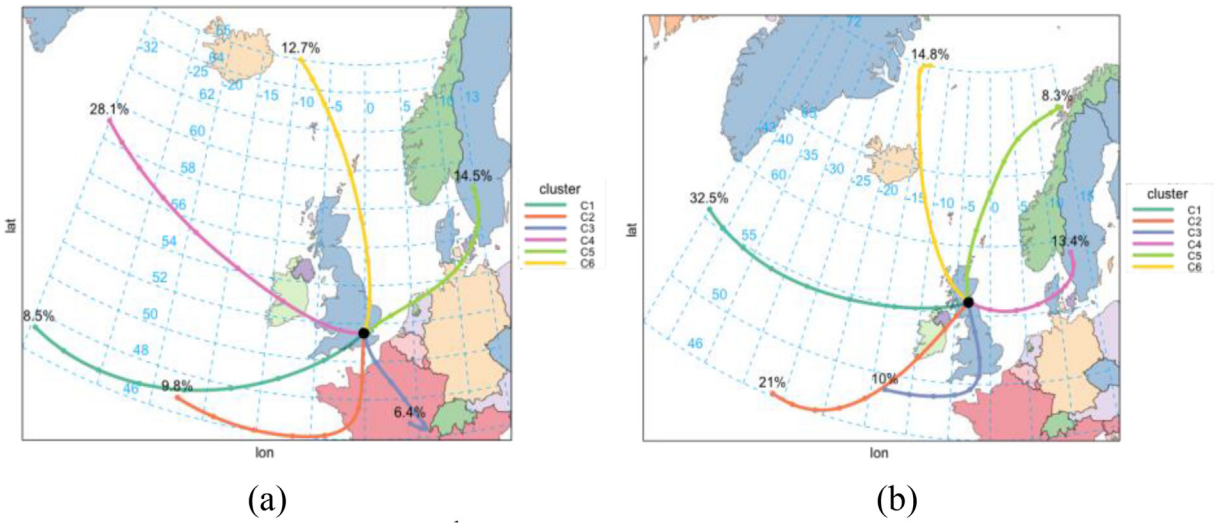

Figure 3. 6-cluster back trajectories[1] for London (panel a) and Edinburg (panel b). The mean trajectory for each cluster.

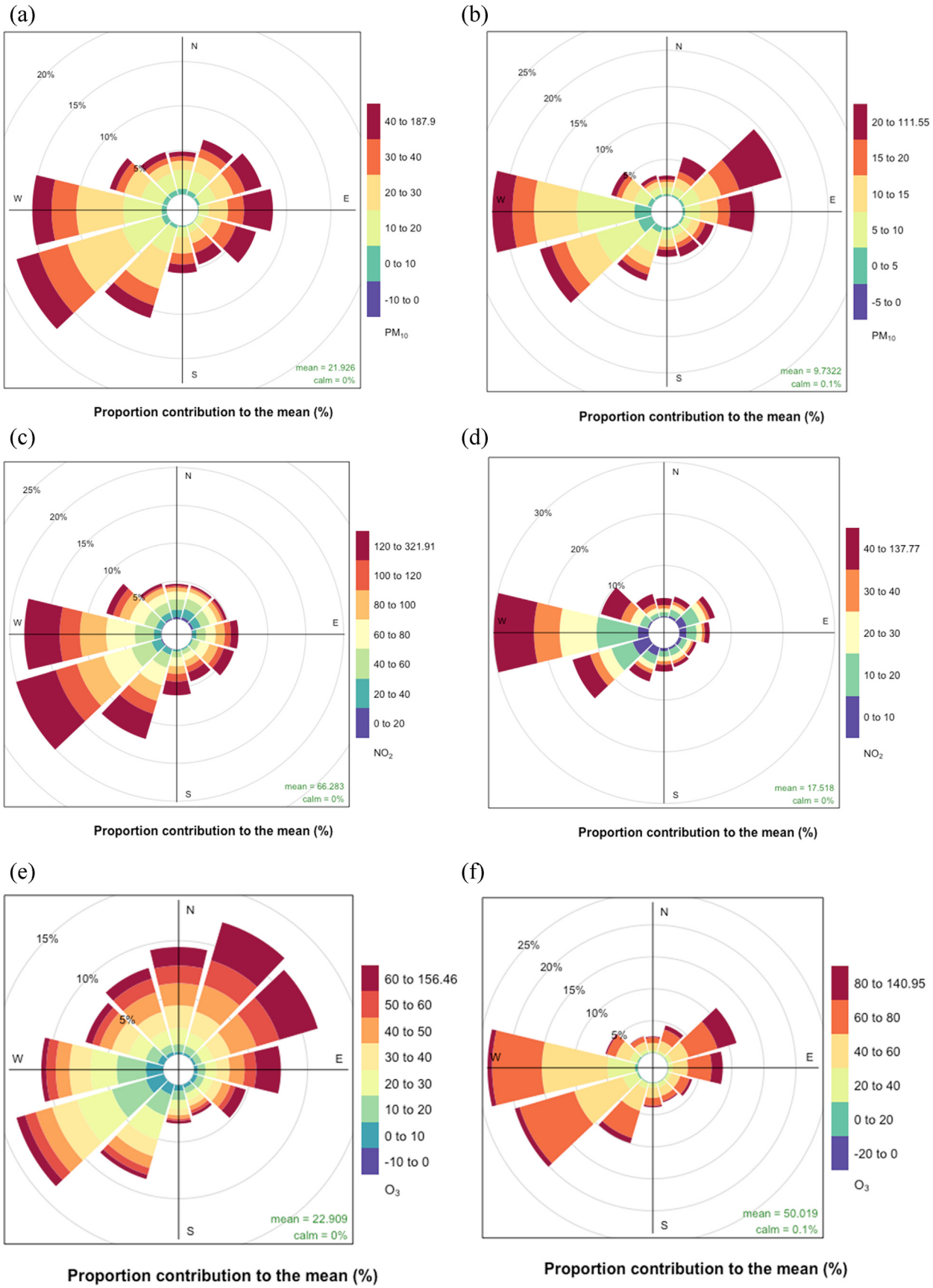

Figure 4. Pollution rose plots for the 2016–2022 period: PM10 in London (panel a) and in Edinburgh (panel b), NO_2 in London (panel c) and in Edinburgh (panel d), O_3 in London (panel e) and in Edinburgh (panel f).

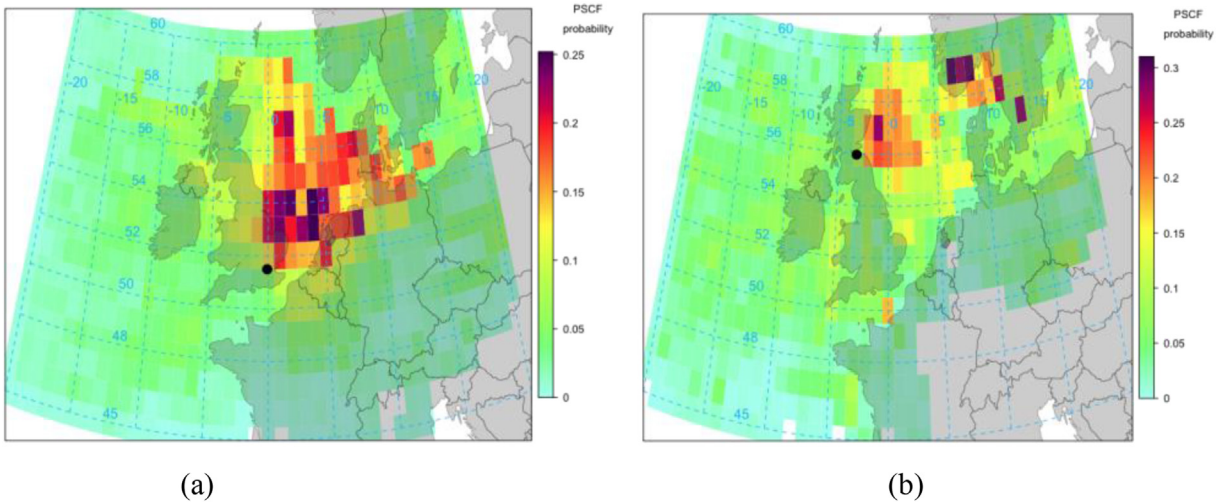

Figure 5. PSCF probabilities (90th percentile) for ozone concentrations in London (panel a) and Edinburgh (panel b).

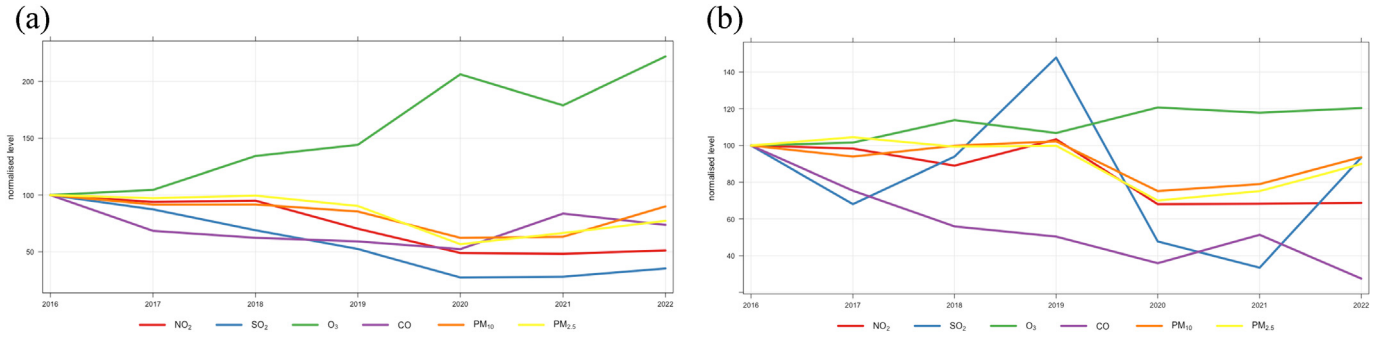

Figure 6. Trends of normalised pollutant data over 2016–2022: London (panel a) and Edinburgh (panel b). The time series index is set to 100 at the beginning of 2016.

concentrations of air pollutants in the two urban areas and the 95% confidence intervals based on resampling methods. Of note, the slope coefficients are expressed in percentage changes and seasonal decomposition is accomplished by loess.

The printed results show that in both geographies the only increasing trend is found for O_3, which registers an average of 19.33% annual increase in London over the entire period, whereas in Edinburgh the concentrations of O_3 registered a rise of 2.83% on average per year over the 2016–2022 period. It should also be mentioned that the positive slope coefficients are significant at the 0.001 level in both cities. On the other hand, in London, the concentrations of SO_2 and NO_2 decreased the most over the seven years, with negative slope coefficients of -13.84% and -9.61%, respectively, significant at 0.001 in both cases. In Edinburgh, the criteria pollutants that have decreased the most are CO (slope of -10.47%, significant at 0.001) and SO_2 (slope of -7.71%, significant at 0.001). Findings also indicate that for all pollutants, with the exception of CO, London registers higher decreases than Edinburg over the analysis period. Most importantly, it should be acknowledged that the Theil-Sen trend analysis is not significantly influenced by the pandemic period. Thus, as Figure 6 previously revealed, with the possible exception of SO2 in the case of Edinburgh, 2020) did not see significant evolutions in pollutant concentrations in the two geographies and consequently cannot be considered an outlier that is capable of distorting long-term trend estimations. Moreover, despite registering significant decay through the first pandemic wave, London ozone concentrations still show an overall positive and significant trend coefficient over the 2016–2022 period, which further reinforces the conclusion that the UK capital registers a strong 7-year trend despite its reversal through 2020.

Generalized Additive Models (GAMs) are further estimated to assure the robustness of the trend analysis for ozone in the two UK capital cities. As previously noted, O_3 is the only criteria pollutant found to exhibit significant increases over the entire sample in both geographies. Table 3 summarizes the estimation results.

In both cases, the corresponding GAM is able to explain much of the variations in O3 concentrations, with an adjusted-R squared of over 81% for the London model and 66% for the Edinburgh model, respectively. The deviance explanation rates have similar values, indicating an excellent fit. The relation between the explanatory and the response variable is linear when the df is close to 1 and nonlinear when the df is >1 (Cheng et al., 2021). Here, estimation results indicate that the relationship between O3 concentrations and time and seasonal variables is highly non-linear in London, whereas for Edinburgh the seasonal component is also nonlinear, while the trend coefficient is closer to 1, suggesting a linear relationship. Also, the coefficients for the smoothed trend and seasonal components are highly statistically significant in all specifications. Moreover, diagnostic tests (available upon request) confirm that the London GAM model is correctly specified, whereas there is still residual correlation in the Edinburgh model. Hence, care should be given when making inferences from the Edinburgh GAM model, whereas more confidence accompanies the London Generalized Additive Model estimation results.

The visual representation of the trend component of the two GAMs (Figure 8(a,b)) confirms that O3 concentrations have registered an increasing trend over the 7-year period in London (panel a) and Edinburgh (panel b), whereas the graphical representation of the seasonal

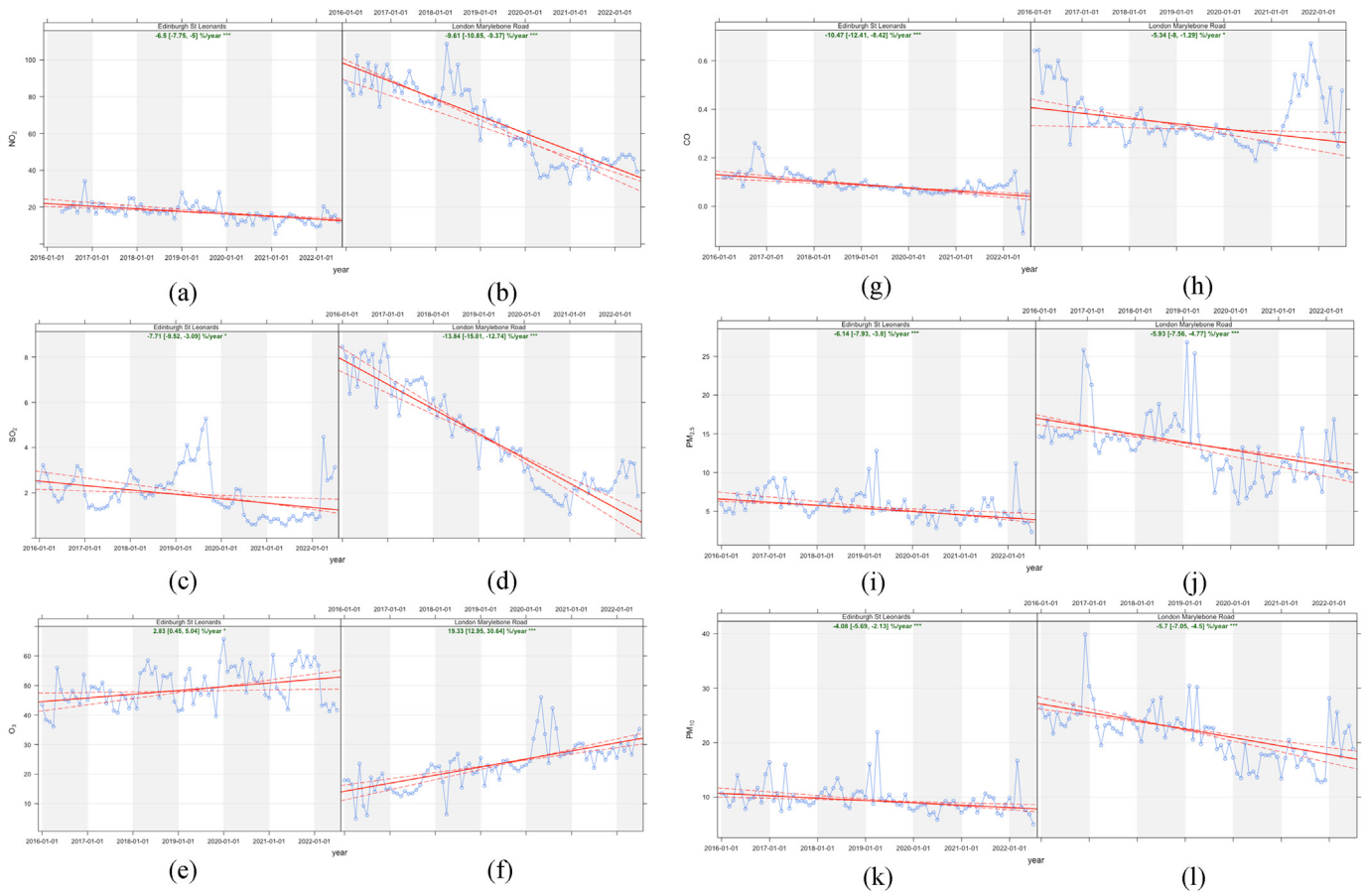

Figure 7. Theil-Sen trend estimations for de-seasonalised criteria pollutants series in Edinburgh and London during 2016–2022: NO2 in Edinburgh (panel a) and London (panel b), SO2 in Edinburgh (panel c) and London (panel d), O3 in Edinburgh (panel e) and London (panel f), CO in Edinburgh (panel g) and London (panel h), PM2.5 in Edinburgh (panel i) and London (panel j), PM10 in Edinburgh (panel k) and London (panel l); seasonal adjustment of trend (i.e. seasonal decomposition by loess) is performed; slope coefficients are expressed in percentage changes; bootstrap resampling is accomplished.

Table 3. Generalized Additive Model (GAM) estimation results.

Estimate[1]	Edf[2] London	Edf Edinburgh
trend	7.14***	1.41**
month	4.91***	5.53***
Adjusted R-squared	0.816	0.664
Deviance explained	0.82	0.67

Note: [1]a cyclic spline is set for the monthly component in GAMs estimation.
[2] The degree of freedom (df) of explanatory variables is selected by the Akaike information criterion (AIC).
** significant at 0.01; *** significant at 0.

component (Figure 9(a,b)) reflects the strong seasonal effect on O3 concentrations that are highest in April–May at both sites.

3.4. COVID-19 impact on ozone pollution

Subsequently, to assess the impact that the COVID-19 imposed lockdown has had on air quality, three distinct widows are delineated within the entire 7-year period, corresponding to a pre-pandemic (i.e., 2016–2019), a pandemic (2020), and a post-pandemic period (2021–2022), respectively. Then, for each window, the trend in the criteria pollutant that registered significant increases over the entire sample in both geographies, i.e., ozone (O3), is estimated. Figure 10 (a-c) contains the graphical representations of the estimation results, while Table 4 summarizes the findings.

Findings reveal that in both urban areas, after adjusting for the seasonal effects, the trend lines show significant reductions in ozone average concentrations during the COVID-19 pandemic period (i.e., during 2020). Trend coefficients have high negative magnitudes and indicate decreases of over 57% in London and approximately 44% (significant at 5%) in Edinburgh during 2020. In the pre-pandemic period (2016–2019), ozone concentrations showed increasing trends in both cities, but of a much higher magnitude in London (15.86% yearly average as compared with 3.23% average yearly increases registered in Edinburg). Furthermore, the trends show a reversal of the decreasing trend and an overall increase of almost 18% yearly average in ozone levels in the post-pandemic period in London, whereas in Edinburgh the pollutant continued its descending trend (−7%) during 2021–2022.

3.5. Diel and seasonal variations of O3

Figure 11 (a,b) complements the previous trend analysis with important information pertaining to O_3 concentration variation that hasn't been detected previously.

This section helps to clarify the (seemingly) divergent results relative to the previous evidence on London air quality changes in the aftermath of the COVID-19 pandemic outbreak. Thus, the graphical depiction shows that, although ozone concentrations have overall decreased by the end of the first pandemic year, i.e. 2020, immediately after the pandemic outbreak and throughout the first pandemic wave, hourly ozone concentrations, as well as average ozone daily and monthly concentrations, have actually risen significantly. This in turn implies that trend

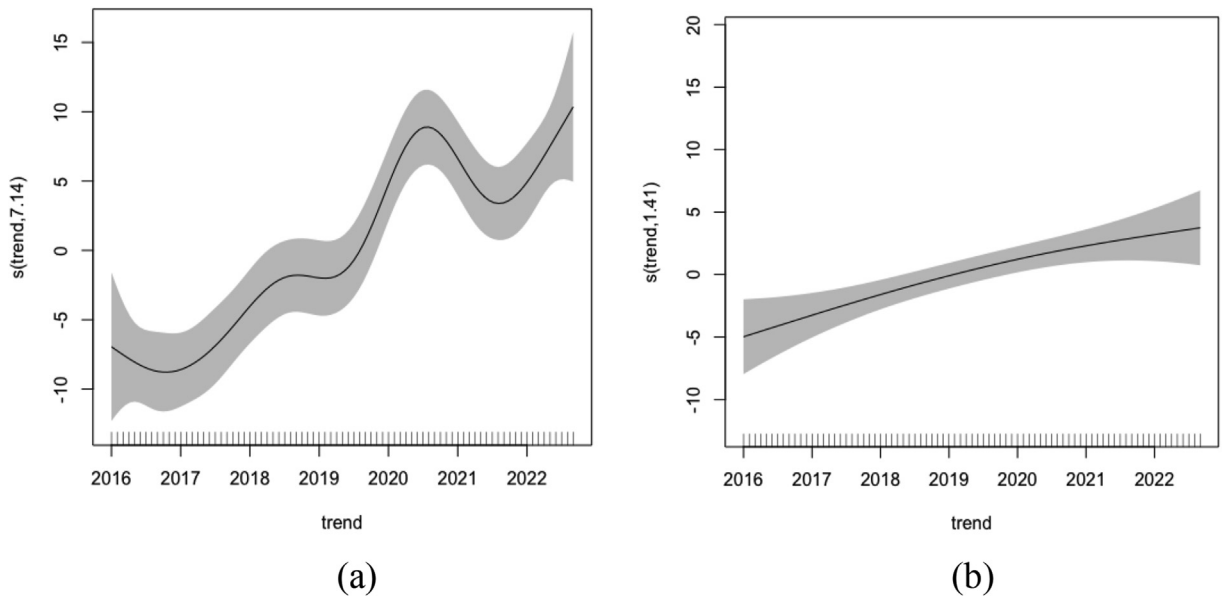

Figure 8. The trend component of the Generalized Additive Model in London (panel a) and Edinburgh (panel b).

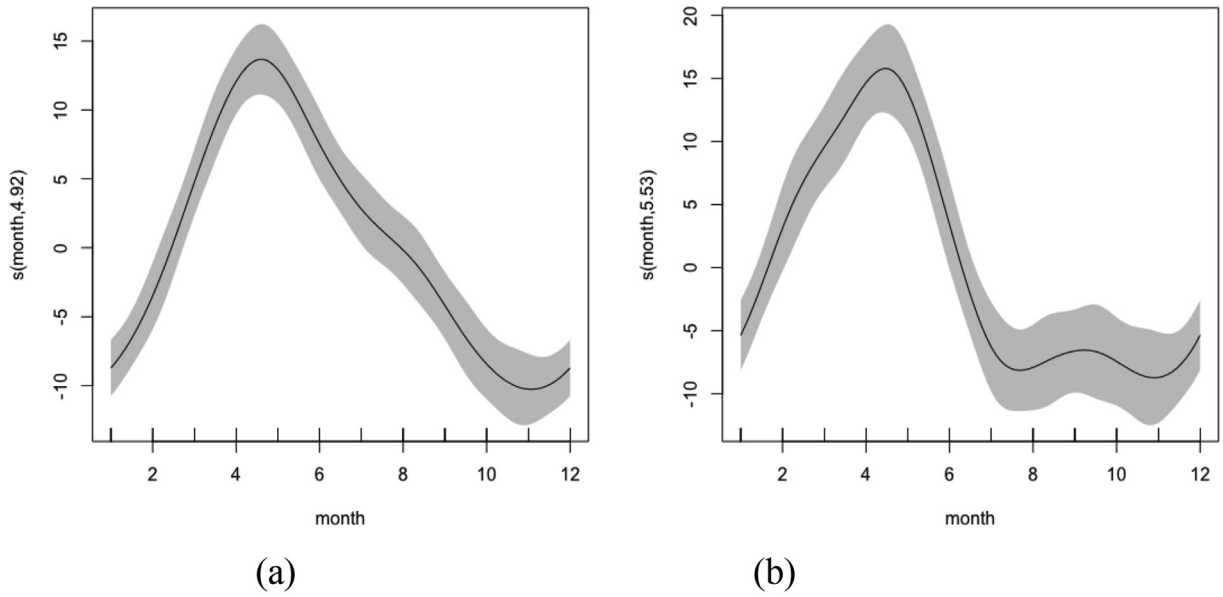

Figure 9. The seasonal component of the Generalized Additive Model in London (panel a) and Edinburgh (panel b).

estimations are significantly influenced by the data splitting strategy and, in particular, the delineation of the "pandemic" timeframe.

The hourly variations, reflected in the hour of the week plots and the diel pattern plots, show similar behaviors in the three sample periods. The O3 concentration pattern across the days of the week is similar in London during the pre and post-pandemic periods but shows a slightly different behavior during 2020, when, unlike for the other periods, rises in the concentrations are seen on Tuesday and Thursday. In both urban areas, higher O3 is registered on weekends over all windows, which is linked to lower NOx emissions in VOC-limited regimes. The occurrence of the "weekend effect" reveals that both sites remain in the NOx-saturated regime throughout all analysis periods. Overall, during the first UK lockdown period imposed on March 23, 2020, sharp increases in O3 concentrations were registered in both UK urban centers compared to the corresponding 2016–2019 levels. Generally, both areas show an annual cycle with low ozone in winter and higher ozone in May.

4. Discussion

Results for London and Edinburgh show that over the 2016–2022 time span, whereas all other air pollutants (i.e., PM10, PM2.5, NO2, CO, and SO2) present decreasing trends, the annual average O3 concentration has increased in the two UK urban sites, with ozone levels in London showing a significant annual increase rate of over 19%, whereas in Edinburgh the registered increasing trend is much lower (i.e., almost 3%). These results deviate from those reported by Sicard et al. (2020a,b), which found that O3 levels decreased in the United Kingdom from 2005 to 2014, and in turn complement the previous findings by showing a reversal in O3 pollution trends in the country during the last seven years. Of note, given that meteorology has a significant impact on the air quality in given geographical areas (Sathe et al., 2021), our estimations confirmed that meteorological factors do not show significant yearly discrepancies over the analyzed period.

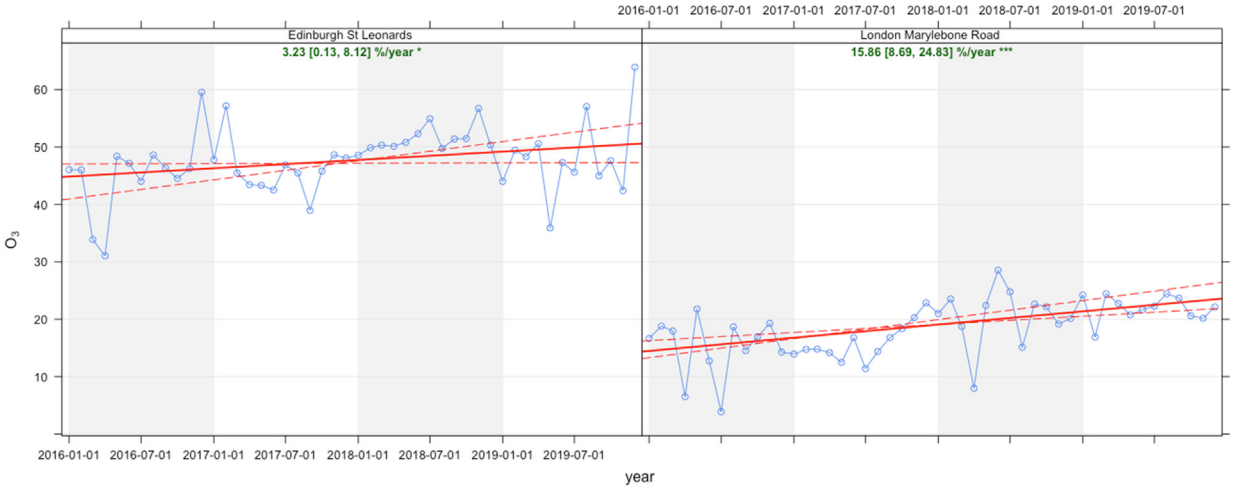

(a)

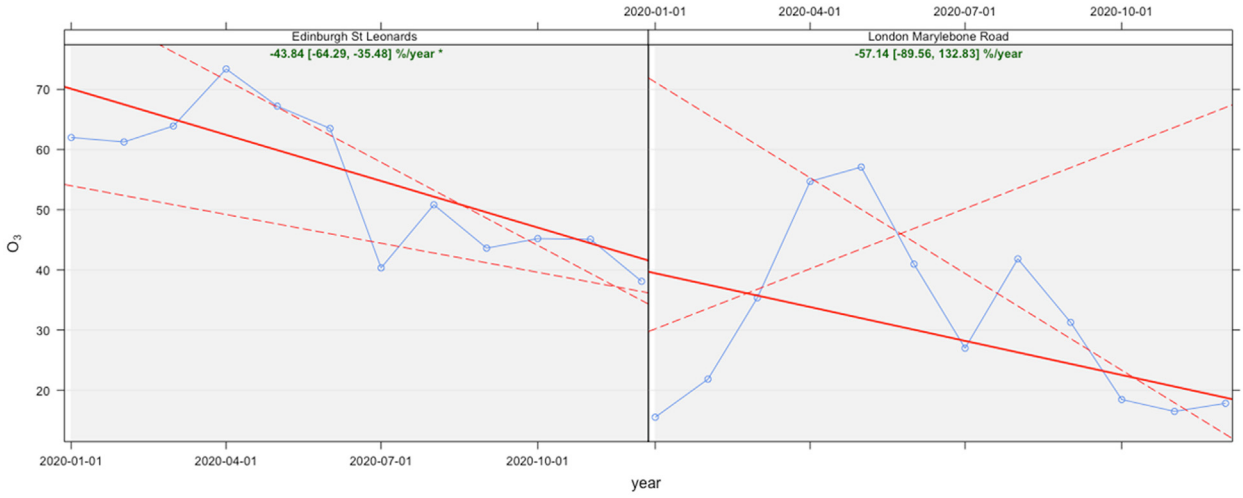

(b)

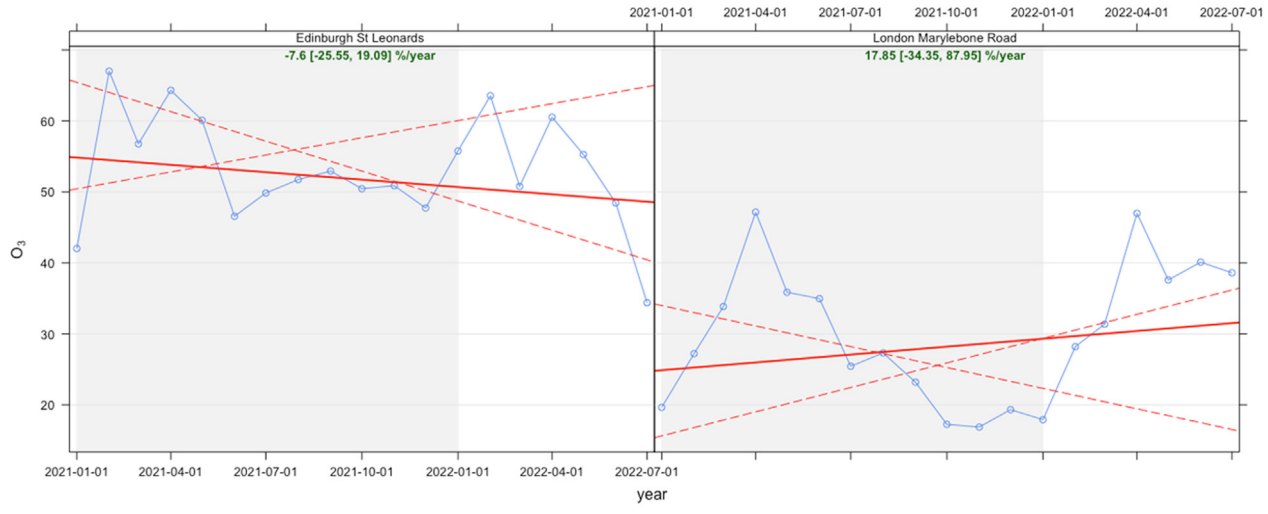

(c)

Figure 10. Theil-Sen trend estimations for ozone concentrations in London and Edinburgh, over three separate windows: pre-pandemic (panel a), pandemic (panel b), and post-pandemic (panel c); seasonal adjustment of trend ((i.e. seasonal decomposition by loess) is performed; slope coefficients are expressed in percentage changes; bootstrap resampling is accomplished.

Table 4. Theil-Sen slope estimates (%) and Mann-Kendall tests for trend (ozone concentrations) in London and Edinburgh.

Site	Whole period (2016–2022)	Pre-pandemic window (2016–2019)	Pandemic window (2020)	Post-pandemic window (2021–2022)
London Marylebone Road	19.33***	15.86***	-57.14	+17.85
Edinburgh St Leonards	2.83**	3.23*	-43.84*	-7.6

NOTE: Deseasoned data with the "stl" function (seasonal trend decomposition using loess); when calling the function, missing data are imputed using a Kalman filter and Kalman smooth. Parameters are estimated through bootstrap resampling, which assures the robustness of results.
*** denotes significance at 0.001; ** denotes significance at 0.01; * denotes significance at 0.05.

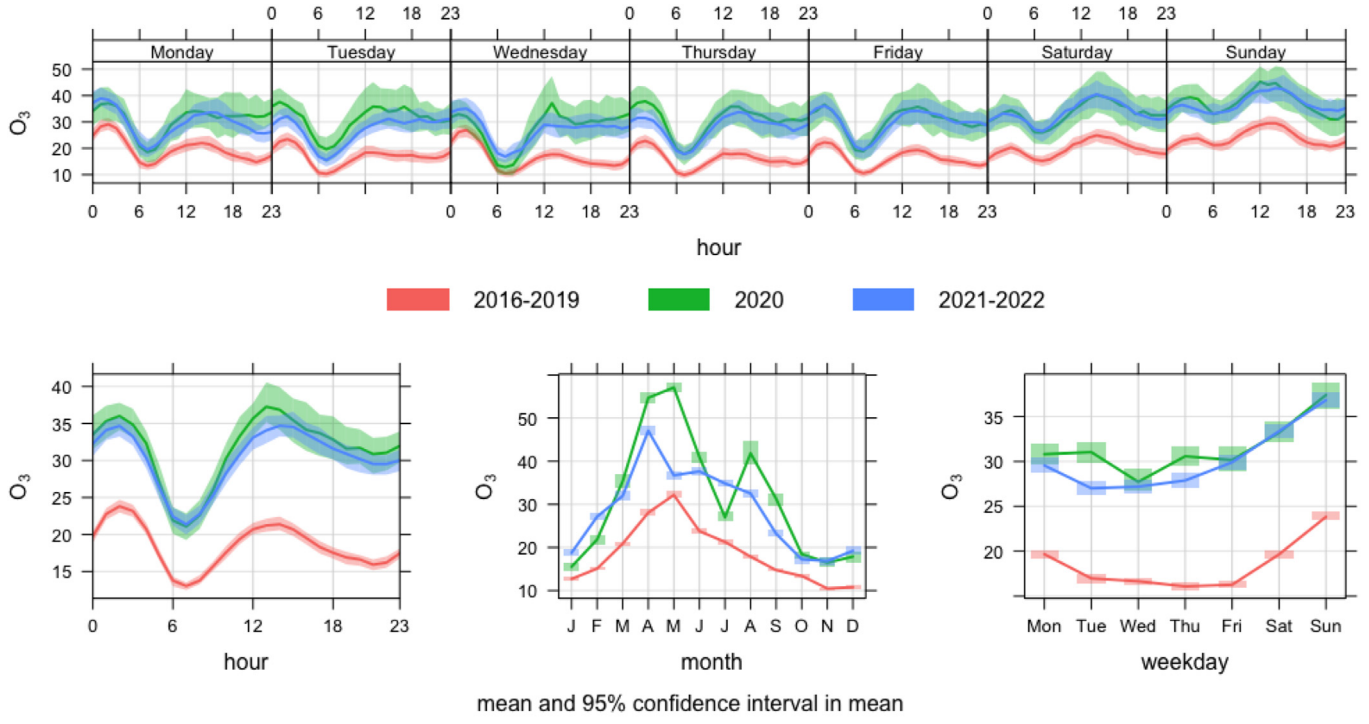

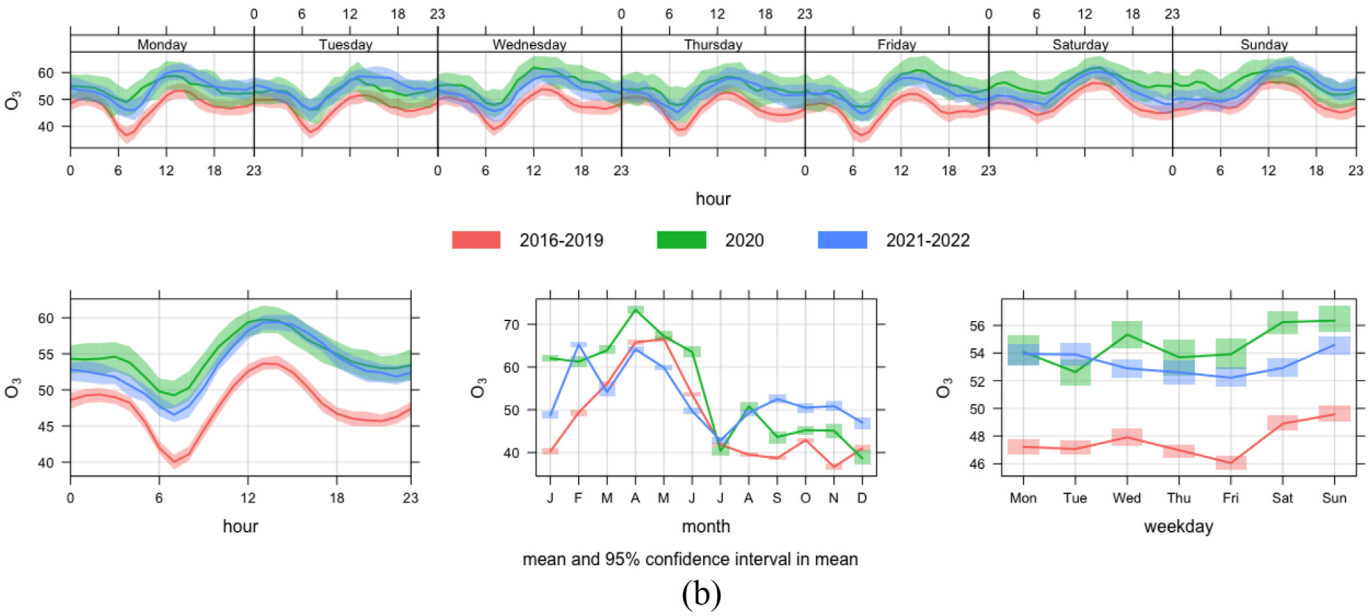

Figure 11. Comparative hourly, daily, weekly, and monthly variations of O3 concentration in London (a) and Edinburgh (b) in three windows: 2016–2019 (red color), 2020 (green color), and 2021–2022 (blue color).

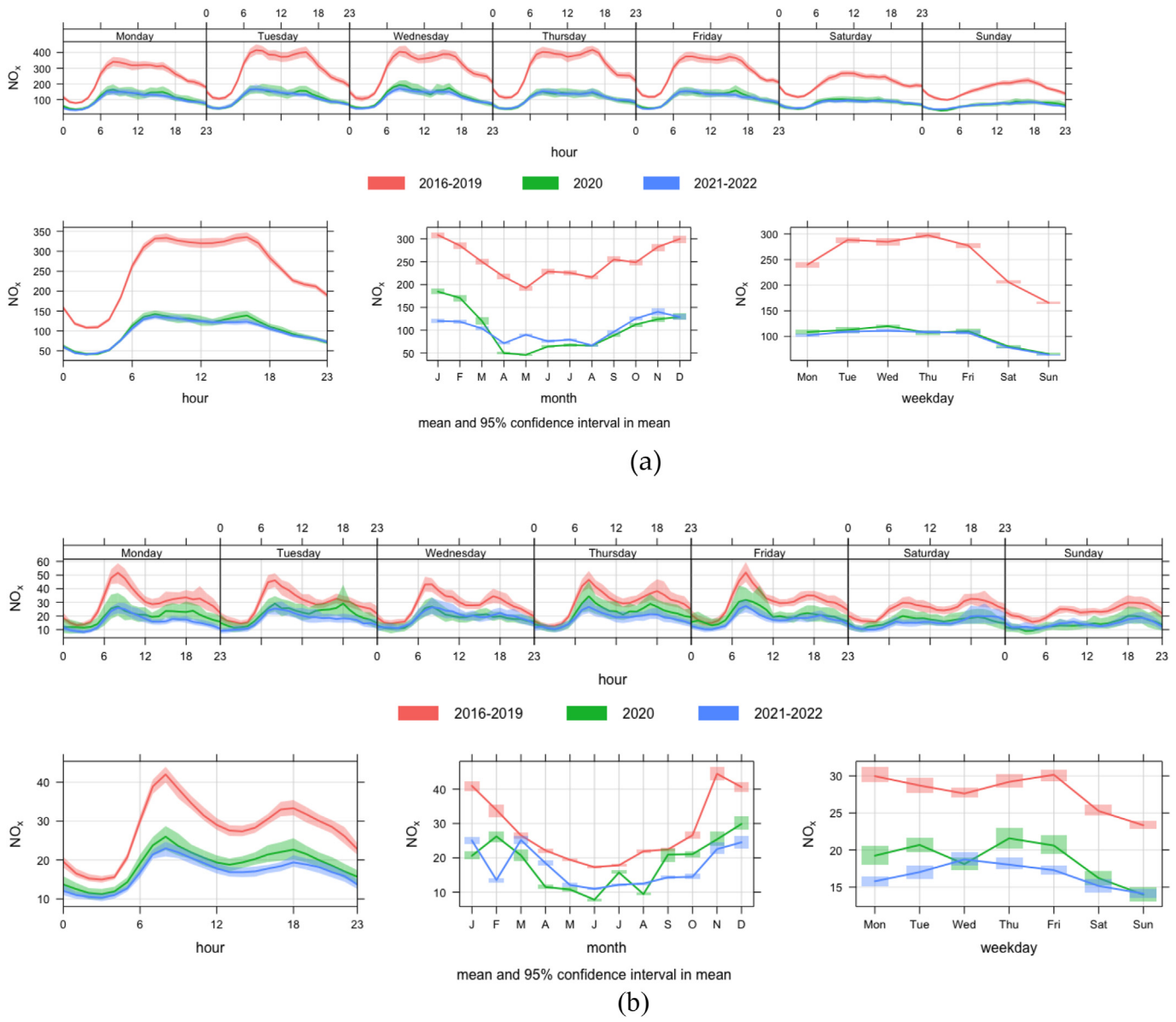

Figure 12. Comparative hourly, daily, weekly, and monthly variations of NOx concentration in London (a) and Edinburgh (b) in three windows: 2016–2019 (red color), 2020 (green color), and 2021–2022 (blue color).

Other important findings reveal that O3 levels have been spurred during the first UK COVID-19 lockdown period, resulting in more severe O3 pollution from March to June 2020 in London and Edinburgh. However, the analysis of both long-term trends and the COVID-19 pandemic impact on O3 concentrations in the two UK urban areas should be conducted with care and should acknowledge that the concentration of secondary pollutants is impacted by complicated nonlinear atmospheric chemistry, involving NOx and volatile organic compound emissions (Zhao et al., 2018; Zhang and Stevenson, 2022). Current results are fully in line with Lee et al. (2020) and Zhang and Stevenson (2022) and indicate that the O3 generation process is in the VOCs-limited regime in both UK urban areas. Thus, the policy implications of current findings should be seen in the light of previous evidence that links NOx mitigation to increased ozone pollution in similar O3 regimes, such as various sites in China (Li et al., 2019a; Ma et al., 2016; Sun et al., 2016). This result is also in line with the findings of other studies that report similar increases in O3 in the aftermath of the pandemic outbreak and subsequent lockdown measures imposed by governments to control its spread, such as Petetin et al. (2020) and Tobias et al. (2020) in various Spanish cities, Sicard et al. (2020a,b) in Rome, Turin, and Nice, Xu et al. (2020) for three Chinese urban centers, and Gopikrishnan et al. (2022) for 8 cities in India. This is particularly important given that ozone is a greenhouse gas (GHG) that has the third largest impact on global warming, surpassed only by carbon dioxide (CO2) and methane (CH4) (Lee et al., 2014). Additionally, ozone significantly affects human health (Zhang et al., 2019; Zhang et al., 2019), having a negative impact, especially on respiratory and cardiovascular systems (Nuvolone et al., 2018). Moreover, the negative impact of ozone on human health is independent of other pollutants (Cohen et al., 2017), which increases both its risk and the necessity to control it through implementing effective policies. Generally, this line of research concludes that ozone pollution has the potential to become a significant issue in NOx-saturated regimes as ambitious policies to mitigate NOx emissions are implemented. Consequently, these studies generally argue that the tradeoff between NOx reduction and O3 increase should be considered in pollution abatement policies in these regimes and indicate that effective and efficient measures should target VOC control. This conclusion is also reached by Li et al. (2019b) and Le et al. (2020) in the case of China. In turn,

previous findings, despite reporting transient evolutions, can have longer-lasting effects on policy (Blackman et al., 2021), which is why a thorough analysis of the pandemic impact, including its longer-range effects, is needed.

Thus, it should be highlighted that most studies that report increased O3 levels during the first pandemic wave generally do not assess the longer-term evolution of ozone pollution. Hence, perhaps most importantly, current findings further indicate a reversal of the increasing trend once the first UK lockdown period ended and activity resumed. Consequently, current results indicate an overall decreasing trend in ozone concentrations during the entire first pandemic year, similar to the findings of recent research (among others, Bekbulat et al., 2021; Miyazaki et al., 2021; Sathe et al., 2021; Querol et al., 2021). Moreover, current findings fully support the conclusions of Tavella and da Silva Júnior (2021) that provide relevant details on the process of ozone formation, showing that, if pandemic-related measures are maintained for periods longer than a few weeks, it is expected to observe diminishing ozone levels even in VOC-controlled geographies (i.e., large urban or metropolitan areas).

Our data further backs this assertion by showing that NOx levels have been well reduced throughout the entire year 2020 in both cities relative to the corresponding pre-pandemic levels, with a consistent difference between average monthly O3 concentrations in the pandemic and the pre-pandemic period (Figure 12(a,b)).

Furthermore, along with chemistry, transport plays a pivotal role in determining local ozone (O3) concentrations (Weber et al., 2020), especially in NOx-saturated coastal regions (Lien and Hung, 2021). Current results highlight that the O3 concentrations in Edinburgh are increased when the trajectories originate in Northern Europe, and O3 concentrations in London are also positively impacted by trajectories originating in mainland Europe (i.e., the Benelux countries). Consequently, the study resonates with NASA (2021) by offering evidence that policy and measures implemented to decrease NOx locally can improve air quality globally. However, as is the case with most research, the current study does suffer from some limitations. Consequently, it should be noted that the study has focused on the pandemic's impact on ozone pollution, neglecting other aspects of lockdown-related air quality changes. Additionally, whereas the evolution of O3 in relation to NOx in the aftermath of the pandemic outbreak has been analyzed, the changes in the VOCs/NOx ratio are also relevant and contribute to explaining evolutions in ozone pollution. Future research can consider these issues.

5. Conclusions

Air pollution is the most serious environmental health issue in the United Kingdom, while Central London is currently the most important geography failing to meet the legally binding limits for main air pollutants imposed at the EU level. On the contrary, Scotland reports on average superior air quality to England and the rest of the United Kingdom, although the capital city, Edinburgh, still exceeds the target limit concentration for some pollutants and ranks second to worst among major European cities in terms of air pollution improvements. Air quality data with high temporal and spatial resolutions are indispensable for relevant and timely research on the characterization, estimation, and prediction of air pollutants, which could in turn assist policymakers to identify efficient policies and control measures to improve air quality and ultimately mitigate pollution-caused health problems and economic costs.

The COVID-19 pandemic has had a positive effect on air quality (EEA, 2021) and consequently constitutes a unique opportunity to assess the extent to which the control of pollution sources contributes to increased air quality in agglomerated urban centers.

The main findings can be summarized as follows: (i) all criteria pollutants (i.e. (PM10, PM2.5, SO2, NO2, and CO) show a decreasing trend over the most recent seven-year period (2016–2022) in Central London and Edinburgh, with the exception of ozone (O3), which presents a significant ascending trend in London and a milder ascending trend in Edinburgh; (ii) over the pandemic period (i.e. during the entire year 2020), O3 concentrations show an overall significant negative trend in both geographies, although during the first pandemic wave (March–June 2020), hourly, daily, and monthly ozone concentrations have risen significantly; (iii) the wind and pollution rose plots confirm that yearly meteorological conditions have been similar over the analysis period, and consequently cannot be considered an influencing factor for trend estimation results; (iv) the cluster analysis of back trajectories performed with the NOAA HYSPLIT model provides important information on air mass origins, indicating that the majority of the back trajectories originated from the Atlantic over the analysis period, with northern Europe identified as a secondary significant source; (v) ozone concentrations show high variations per cluster, particularly in London, and the clusters originating from northern Europe are associated with the highest concentrations of ozone in both locations. This finding is additionally reinforced through pollution rose plots analysis; (vi) the analysis of the Potential Source Contribution Function (PSCF) confirms that principal ozone sources are dominated by source origins in northern Europe, particularly Norway and Sweden in the case of Edinburgh, and also mainland Europe (i.e., the Benelux countries) in the case of London.

The study confirms that the O3 generating process is in the VOCs-limited regime in both UK urban areas throughout the seven-year period. However, different from previous research, it shows that ozone pollution is not necessary to become an issue of concern with the implementation of NOx emissions mitigation measures. Moreover, it informs policymakers in London and Edinburgh that both local and transboundary sources contribute to local ozone pollution. Consequently, the analysis of trends and variations at the principal sources is needed to complement the current investigation and could constitute an avenue for future research.

Declarations

Author contribution statement

CRISTIANA TUDOR: Conceived and designed the experiments; Performed the experiments; Analyzed and interpreted the data; Contributed reagents, materials, analysis tools or data; Wrote the paper.

Funding statement

This research did not receive any specific grant from funding agencies in the public, commercial, or not-for-profit sectors.

Data availability statement

Data included in article/supp. material/referenced in article.

Declaration of interest's statement

The authors declare no conflict of interest.

Additional information

No additional information is available for this paper.

Appendix A

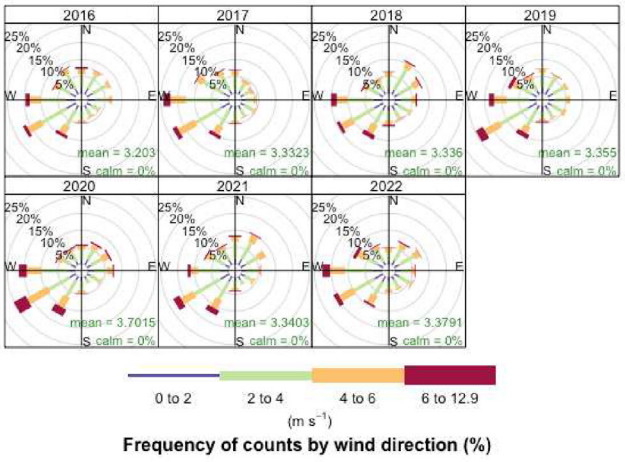

(a)

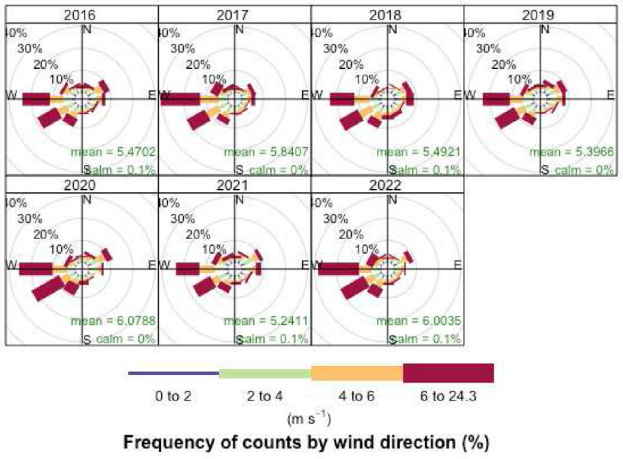

(b)

A1. Wind speed/direction frequencies by year in London (panel a) and Edinburgh (panel b).

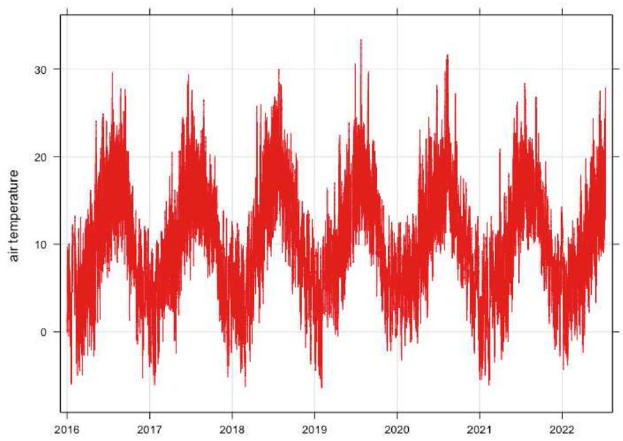

(a)

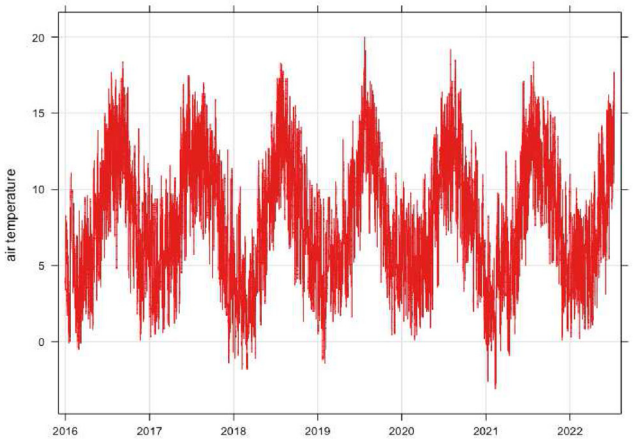

(b)

A2. Variations in temperature over 2016–2022: London (panel a) and Edinburgh (panel b).

References

Air quality news, 2021. 99% of London exceeds WHO air pollution limits. Available at: https://airqualitynews.com/2021/01/25/99-of-london-exceeds-who-air-pollution-limits/. Accessed on June 23rd, 2022.

Ali, R., Kuriqi, A., Abubaker, S., Kisi, O., 2019. Long-term trends and seasonality detection of the observed flow in Yangtze River using Mann-Kendall and Sen's innovative trend method. Water 11 (9), 1855.

Anil, I., Alagha, O., Karaca, F., 2017. Effects of transport patterns on chemical composition of sequential rain samples: trajectory clustering and principal component analysis approach. Air Qual., Atmosp. Health 10 (10), 1193–1206.

Applequist, S., 2012. Wind rose bias correction. J. Appl. Meteorol. Climatol. 51 (7), 1305–1309.

Ashmore, M., 2013. Air Pollution. In: Levin, S.A. (Ed.), Encyclopedia of Biodiversity. Elsevier Inc.

Balamurugan, V., Balamurugan, V., Chen, J., 2022. Importance of ozone precursors information in modelling urban surface ozone variability using machine learning algorithm. Sci. Rep. 12 (1), 1–8.

Bekbulat, B., Apte, J.S., Millet, D.B., Robinson, A.L., Wells, K.C., Presto, A.A., Marshall, J.D., 2021. Changes in criteria air pollution levels in the US before, during, and after Covid-19 stay-at-home orders: evidence from regulatory monitors. Sci. Total Environ. 769, 144693.

Blackman, A., Bonilla, J.A., Villalobos, L., 2021. Quantifying COVID-19's silver lining: avoided deaths from air quality improvements in Bogotá (No. IDB-WP-1270). IDB Working Paper Series.

Bodor, Z., Bodor, K., Keresztesi, Á., Szép, R., 2020. Major air pollutants seasonal variation analysis and long-range transport of PM10 in an urban environment with specific climate condition in Transylvania (Romania). Environ. Sci. Pollut. Control Ser. 27 (30), 38181–38199.

Boubel, R.W., Vallero, D., Fox, D.L., Turner, B., Stern, A.C., 2013. Fundamentals of Air Pollution. Elsevier.

Campbell, P.C., Tong, D., Tang, Y., Baker, B., Lee, P., Saylor, R., et al., 2021. Impacts of the COVID-19 economic slowdown on ozone pollution in the US. Atmos. Environ. 264, 118713.

Carslaw, D.C., 2022. Openair book. Available at: https://bookdown.org/david_carslaw/openair/. Accessed on: March 20, 2022.

Carslaw, D.C., Ropkins, K., 2012. Openair—an R package for air quality data analysis. Environ. Model. Software 27, 52–61.

Carslaw, D.C., Ropkins, K., 2012. Environmental Modelling & Software 27–28, 52–61 Environment 44 (13), 1682–1690.
Carslaw, D.C., Beevers, S.D., Ropkins, K., Bell, M.C., 2006. Detecting and quantifying aircraft and other on-airport contributions to ambient nitrogen oxides in the vicinity of a large international airport. Atmos. Environ. 40 (28), 5424e5434.
Centre for Cities, 2020. Cities outlook 2020. Available online: https://smartthinking.org.uk/cities-outlook-2020/. Accessed on April 10, 2022.
Chen, Z., Liu, J., Qie, X., Cheng, X., Shen, Y., Yang, M., et al., 2022. Transport of substantial stratospheric ozone to the surface by a dying typhoon and shallow convection. Atmos. Chem. Phys. 22 (12), 8221–8240.
Cheng, B., Ma, Y., Feng, F., Zhang, Y., Shen, J., Wang, H., et al., 2021. Influence of weather and air pollution on concentration change of PM2. 5 using a generalized additive model and gradient boosting machine. Atmos. Environ. 255, 118437.
Cleveland, R.B., Cleveland, W.S., McRae, J.E., Terpenning, I., 1990. STL: a seasonal-trend decomposition procedure based on loess. J. Off. Stat. 6, 3–73.
CNN, 2020. Air pollution falls by unprecedented levels in major global cities during coronavirus lockdowns. Available at: https://edition.cnn.com/2020/04/22/world/air-pollution-reduction-cities-coronavirus-intl-hnk/index.html. accessed on 15 September 2022.
Dantas, G., Siciliano, B., Freitas, L., de Seixas, E.G., da Silva, C.M., Arbilla, G., 2019. Why did ozone levels remain high in Rio de Janeiro during the Brazilian truck driver strike? Atmos. Pollut. Res. 10 (6), 2018–2029.
Dantas, G., Siciliano, B., França, B.B., da Silva, C.M., Arbilla, G., 2020. The impact of COVID-19 partial lockdown on the air quality of the city of Rio de Janeiro, Brazil. Sci. Total Environ. 729, 139085.
Dominici, F., McDermott, A., Zeger, S.L., Samet, J.M., 2002. On the use of generalized additive models in time-series studies of air pollution and health. Am. J. Epidemiol. 156 (3), 193–203.
dos Santos, O.N., Hoinaski, L., 2021. Incorporating gridded concentration data in air pollution back trajectories analysis for source identification. Atmos. Res. 263, 105820.
Droppo, J.G., Napier, B.A., 2008. Wind direction bias in generating wind roses and conducting sector-based air dispersion modeling. J. Air Waste Manag. Assoc. 58 (7), 913–918.
Earth Lab, 2022. Creating interactive spatial maps in R using leaflet. Available online: https://www.earthdatascience.org/courses/earth-analytics/get-data-using-apis/leaflet-r/. Accessed on June 30th, 2022.
Environmental Protection Agency (EPA), 2021. What is ozone and where is it in the atmosphere? Available at: https://www.epa.gov/ozone-pollution-and-your-patients-health/what-ozone. accessed on July 2nd , 2022.
Environmental Protection Agency (EPA), 2022. Trends in ozone adjusted for weather conditions. Available at: https://www.epa.gov/air-trends/trends-ozone-adjusted-weather-conditions. accessed on July 1st, 2022.
European Environment Agency (EEA), 2021. Europe's Air Quality Status 2021. Available at: https://www.eea.europa.eu/publications/air-quality-status-2021. Accessed on July 4th, 2022.
European Environment Agency (EEA). Available at: https://www.eea.europa.eu/themes/air/air-quality/resources/glossary/ozone-precursor. accessed on July 1st, 2022.
Fino, A., 2019. Air quality legislation. In: Nriagu, J.O. (Ed.), Encyclopedia of Environmental Health. Elsevier.
Gopikrishnan, G.S., Kuttippurath, J., Raj, S., Singh, A., Abbhishek, K., 2022. Air quality during the COVID–19 lockdown and unlock periods in India analyzed using satellite and ground-based measurements. Environ. Process. 9 (2), 1–21.
Hao, T., Cai, Z., Chen, S., Han, S., Yao, Q., Fan, W., 2019. Transport pathways and potential source regions of PM2.5 on the west coast of bohai bay during 2009–2018. Atmosphere 10.
Henry, R., Norris, G.A., Vedantham, R., Turner, J.R., 2009. Source region identification using kernel smoothing. Environ. Sci. Technol. 43 (11), 4090–4097.
IQAir, 2022. Air quality in United Kingdom. Available online: https://www.iqair.com/us/uk. Accessed on April 10, 2022.
Jacob, D.J., Winner, D.A., 2009. Effect of climate change on air quality. Atmos. Environ. 43 (1), 51–63.
Jeong, U., Kim, J., Lee, H., Jung, J., Kim, Y.J., Song, C.H., Koo, J.H., 2011. Estimation of the contributions of long range transported aerosol in East Asia to carbonaceous aerosol and PM concentrations in Seoul, Korea using highly time resolved measurements: a PSCF model approach. J. Environ. Monit. 13 (7), 1905–1918.
Jones, A.M., Harrison, R.M., Baker, J., 2010. The wind speed dependence of the concentrations of airborne particulate matter and NOx. Atmos. Environ. 44 (13), 1682–1690.
Lee, Y.C., Shindell, D.T., Faluvegi, G., Wenig, M., Lam, Y.F., Ning, Z., et al., 2014. Increase of ozone concentrations, its temperature sensitivity and the precursor factor in South China. Tellus B 66 (1), 23455.
Lee, M., Brauer, M., Wong, P., Tang, R., Tsui, T.H., Choi, C., et al., 2017. Land use regression modelling of air pollution in high density high rise cities: a case study in Hong Kong. Sci. Total Environ. 592, 306–315.
Lien, J., Hung, H.M., 2021. The contribution of transport and chemical processes on coastal ozone and emission control strategies to reduce ozone. Heliyon 7 (10), e08210.
Lois, E., Keating, E.L., Gupta, A.K., 2002. Fuels. In: Meyers, R.A. (Ed.), Encyclopedia of Physical Science and Technology. Academic Press.
London Air, 2022. Is air pollution worse in London? Available at: https://www.londonair.org.uk/londonair/guide/London.aspx. Accessed on June 22, 2022.
Mahato, S., Pal, S., Ghosh, K.G., 2020. Effect of lockdown amid COVID-19 pandemic on air quality of the megacity Delhi, India. Sci. Total Environ. 730, 139086.
Makra, L., Ionel, I., Csépe, Z., Matyasovszky, I., Lontis, N., Popescu, F., Sümeghy, Z., 2013. The effect of different transport modes on urban PM10 levels in two European cities. Sci. Total Environ. 458, 36–46.
Manisalidis, I., Stavropoulou, E., Stavropoulos, A., Bezirtzoglou, E., 2020. Environmental and health impacts of air pollution: a review. Front. Public Health 14.
Mendes, L., Monjardino, J., Ferreira, F., 2022. Air quality forecast by statistical methods: application to Portugal and Macao. Front. Big Data 5.
Miyazaki, K., Bowman, K., Sekiya, T., Takigawa, M., Neu, J.L., Sudo, K., et al., 2021. Global tropospheric ozone responses to reduced NO x emissions linked to the COVID-19 worldwide lockdowns. Sci. Adv. 7 (24), eabf7460.
Munn, R.E., 1969. Pollution wind-rose analysis. Atmosphere 7 (3), 97–105.
Myllyvirta, L., Thieriot, H., 2020. 11,000 air pollution-related deaths avoided in Europe as coal, oil consumption plummet. Available in: https://energyandcleanair.org/wp/wp-content/uploads/2020/04/CREA-Europe-COVID-impacts.pdf (Accessed May 2020).
National Aeronautics and Space Administration (NASA), 2021. Local lockdowns brought fast global ozone reductions, NASA finds. Available at: https://www.nasa.gov/feature/jpl/local-lockdowns-brought-fast-global-ozone-reductions-nasa-finds. Accessed on July 1st, 2022.
New Hampshire Department of Environmental Services (NHDES), 2022. Criteria pollutants. Available online: https://www.des.nh.gov/air/state-implementation-plans/criteria-pollutants. Accessed on April 14, 2022.
Nuvolone, D., Petri, D., Voller, F., 2018. The effects of ozone on human health. Environ. Sci. Pollut. Control Ser. 25 (9), 8074–8088.
Ordóñez, C., Garrido-Perez, J.M., García-Herrera, R., 2020. Early spring near-surface ozone in Europe during the COVID-19 shutdown: meteorological effects outweigh emission changes. Sci. Total Environ. 747, 141322.
Organisation for Economic Co-operation and Development (OECD), 2021. The economic consequences of outdoor air pollution. Available online: https://www.oecd.org/environment/indicators-modelling-outlooks/Policy-Highlights-Economic-consequences-of-outdoor-air-pollution-web.pdf. Accessed on April 14, 2022.
Pey, J., Cerro, J.C., 2022. Reasons for the observed tropospheric ozone weakening over south-western Europe during COVID-19: strict lockdown versus the new normal. Sci. Total Environ. 833, 155162.
Public Health England, 2019. Review of interventions to improve outdoor air quality and public health. Available online: https://assets.publishing.service.gov.uk/government/uploads/system/uploads/attachment_data/file/938623/Review_of_interventions_to_improve_air_quality_March-2019-2018572.pdf. Accessed on April 14, 2022.
Pusede, S.E., Cohen, R.C., 2012. On the observed response of ozone to NO x and VOC reactivity reductions in San Joaquin Valley California 1995–present. Atmos. Chem. Phys. 12 (18), 8323–8339.
Pusede, S.E., Gentner, D.R., Wooldridge, P.J., Browne, E.C., Rollins, A.W., Min, K.E., et al., 2014. On the temperature dependence of organic reactivity, nitrogen oxides, ozone production, and the impact of emission controls in San Joaquin Valley, California. Atmos. Chem. Phys. 14 (7), 3373–3395.
Querol, X., Massagué, J., Alastuey, A., Moreno, T., Gangoiti, G., Mantilla, E., et al., 2021. Lessons from the COVID-19 air pollution decrease in Spain: now what? Sci. Total Environ. 779, 146380.
Rahman, W., Beig, G., Barman, N., Hopke, P.K., Hoque, R.R., 2021. Ambient ozone over mid-Brahmaputra Valley, India: effects of local emissions and atmospheric transport on the photostationary state. Environ. Monit. Assess. 193 (12), 1–17.
Ravindra, K., Rattan, P., Mor, S., Aggarwal, A.N., 2019. Generalized additive models: building evidence of air pollution, climate change and human health. Environ. Int. 132, 104987.
Roubeyrie, L., Celles, S., 2018. Windrose: a Python Matplotlib, Numpy library to manage wind and pollution data, draw windrose. J. Open Source Software 3 (29), 268.
Saadat, S., Rawtani, D., Hussain, C.M., 2020. Environmental perspective of COVID-19. Sci. Total Environ. 728, 138870.
Sathe, Y., Gupta, P., Bawase, M., Lamsal, L., Patadia, F., Thipse, S., 2021. Surface and satellite observations of air pollution in India during COVID-19 lockdown: implication to air quality. Sustain. Cities Soc. 66, 102688.
Sheng, N., Tang, U.W., 2013. Risk assessment of traffic-related air pollution in a world heritage city. Int. J. Environ. Sci. Technol. 10 (1), 11–18.
Sicard, P., De Marco, A., Agathokleous, E., Feng, Z., Xu, X., Paoletti, E., et al., 2020a. Amplified ozone pollution in cities during the COVID-19 lockdown. Sci. Total Environ. 735, 139542.
Sicard, P., Paoletti, E., Agathokleous, E., Araminienė, V., Proietti, C., Coulibaly, F., De Marco, A., 2020b. Ozone weekend effect in cities: deep insights for urban air pollution control. Environ. Res. 191, 110193.
Siciliano, B., Dantas, G., da Silva, C.M., Arbilla, G., 2020. Increased ozone levels during the COVID-19 lockdown: analysis for the city of Rio de Janeiro, Brazil. Sci. Total Environ. 737, 139765.
Sirois, A., Bottenheim, J.W., 1995. Use of backward trajectories to interpret the 5-year record of PAN and O3 ambient air concentrations at Kejimkujik National Park, Nova Scotia. J. Geophys. Res. 100, 2867–2881.
Stein, A.F., Draxler, R.R., Rolph, G.D., Stunder, B.J.B., Cohen, M.D., Ngan, F., 2015. NOAA's HYSPLIT atmospheric transport and dispersion modeling system. Bull. Am. Meteorol. Soc. 96 (12), 2059–2077.
Su, L., Yuan, Z., Fung, J.C., Lau, A.K., 2015. A comparison of HYSPLIT backward trajectories generated from two GDAS datasets. Sci. Total Environ. 506, 527–537.
Sulaymon, I.D., Zhang, Y., Hopke, P.K., Zhang, Y., Hua, J., Mei, X., 2021. COVID-19 pandemic in Wuhan: ambient air quality and the relationships between criteria air pollutants and meteorological variables before, during, and after lockdown. Atmos. Res. 250, 105362.

Tavella, R.A., da Silva Júnior, F.M.R., 2021. Watch out for trends: did ozone increased or decreased during the COVID-19 pandemic? Environ. Sci. Pollut. Control Ser. 28 (47), 67880–67885.

The Association of Directors of Public Health (ADPH), 2017. Policy position: outdoor air quality. Available online: http://www.adph.org.uk/wp-content/uploads/2017/11/ADPH-Policy-Position-Outdoor-Air-Quality.pdf. Accessed on April 17, 2022.

The Scotsman, 2022a. Air pollution: why is air quality bad today and how does Scotland's air quality compare to the rest of the UK? Available online: https://www.scotsman.com/news/environment/air-pollution-why-is-air-quality-bad-today-and-how-does-scotlands-air-quality-compare-to-the-rest-of-the-uk-3625066. Accessed on April 16, 2022.

The Scotsman, 2022b. Edinburgh second worst among leading European cities for air pollution improvements – campaigners Clean Cities. Available online: https://www.scotsman.com/news/transport/edinburgh-second-worst-among-leading-european-cities-for-improving-air-quality-3583228. Accessed on April 16, 2022.

Tobias, A., Carnerero, C., Reche, C., Massague, J., Via, M., Minguillon, M.C., Alastuey, A., Querol, X., 2020. Changes in air quality during the lockdown in Barcelona (Spain) one month into the SARS-CoV-2 epidemic. Sci. Total Environ.

Torkmahalleh, M.A., Akhmetvaliyeva, Z., Omran, A.D., Omran, F.D., Kazemitabar, M., Naseri, M., Xie, S., 2021. Global air quality and COVID-19 pandemic: do we breathe cleaner air? Aerosol Air Qual. Res. 21, 1.

Tudor, C., Sova, R., 2021. Benchmarking GHG emissions forecasting models for global climate policy. Electronics 10 (24), 3149.

Tudor, C., Sova, R., 2022. EU net-zero policy achievement assessment in selected members through automated forecasting algorithms. ISPRS Int. J. Geo-Inf. 11 (4), 232.

UK Legislation: National Emissions Ceiling Regulations. Available at: https://www.legislation.gov.uk/uksi/2018/129/contents/made. Accessed on 19 September 2022.

United Nations (UN), 2021. Improving air quality 'key' to confronting global environmental crises. Available online: https://news.un.org/en/story/2021/09/1099042. Accessed on April 10, 2022.

United Nations Environment Programme (UNEP), 2021. 5 dangerous pollutants you're breathing in every day. Available online: https://www.unep.org/news-and-stories/story/5-dangerous-pollutants-youre-breathing-every-day#:∼:text=Nitrogen%20Dioxide&text=NO2%20is%20the%20most,formation%20of%20ground%2Dlevel%20ozone. Accessed on April 10, 2022.

Vallero, D., 2014. Fundamentals of Air Pollution. Academic Press.

Venter, Z.S., Aunan, K., Chowdhury, S., Lelieveld, J., 2020. COVID-19 lockdowns cause global air pollution declines. Proc. Natl. Acad. Sci. USA 117 (32), 18984–18990.

Wang, Q., Su, M., 2020. A preliminary assessment of the impact of COVID-19 on environment–A case study of China. Sci. Total Environ. 728, 138915.

Washington Post, 2020. The silver lining to coronavirus lockdowns: air quality is improving. Available at: https://www.washingtonpost.com/weather/2020/04/09/air-quality-improving-coronavirus/. Accessed on 16 September 2022.

Weber, J., Shin, Y.M., Staunton Sykes, J., Archer-Nicholls, S., Abraham, N.L., Archibald, A.T., 2020. Minimal climate impacts from short-lived climate forcers following emission reductions related to the COVID-19 pandemic. Geophys. Res. Lett. 47 (20), e2020GL090326.

Westmoreland, E.J., Carslaw, N., Carslaw, D.C., Gillah, A., Bates, E., 2007. Analysis of air quality within a street canyon using statistical and dispersion modelling techniques. Atmos. Environ. 41 (39), 9195e9205.

Wood, S.N., 2017. Generalized Additive Models: an Introduction with R, second ed. Chapman and Hall/CRC Press.

World Economic Forum, 2020. This is the effect coronavirus has had on air pollution all across the world. Available at: https://www.weforum.org/agenda/2020/04/coronavirus-covid19-air-pollution-enviroment-nature-lockdown. Accessed on 15 September 2022.

World Health Organization (WHO), 2021. Ambient (outdoor) air pollution. Available online: https://www.who.int/news-room/fact-sheets/detail/ambient-(outdoor)-air-quality-and-health. Accessed on April 12, 2022.

Wyche, K.P., Nichols, M., Parfitt, H., Beckett, P., Gregg, D.J., Smallbone, K.L., Monks, P.S., 2021. Changes in ambient air quality and atmospheric composition and reactivity in the South East of the UK as a result of the COVID-19 lockdown. Sci. Total Environ. 755, 142526.

Xu, K., Cui, K., Young, L., Hsieh, Y., Wang, Y., Zhang, J., Wan, S., 2020. Impact of the COVID-19 event on air quality in central China. Aerosol Air Qual. Res. 20, 5.

Zhang, C., Stevenson, D., 2022. Characteristic changes of ozone and its precursors in London during COVID-19 lockdown and the ozone surge reason analysis. Atmos. Environ. 273, 118980.

Zhang, J., Chen, Q., Wang, Q., Ding, Z., Sun, H., Xu, Y., 2019. The acute health effects of ozone and PM2. 5 on daily cardiovascular disease mortality: a multi-center time series study in China. Ecotoxicol. Environ. Saf. 174, 218–223.

Natural Resources Conservation Service (NRCS), 2022. ozone precursors and animal operations. Available at: https://www.nrcs.usda.gov/Internet/FSE_DOCUMENTS/stelprdb1043545.pdf. Accessed on July 1, 2022.